Molecular Biology of the Cell
Vol. 17, 3187–3196, July 2006

The Docking Protein Cas Links Tyrosine Phosphorylation Signaling to Elongation of Cerebellar Granule Cell Axons[D]

Jinhong Huang,* Ryuichi Sakai,† and Teiichi Furuichi*

*Laboratory for Molecular Neurogenesis, Riken Brain Science Institute, Wako, Saitama 351-0198; and †Growth Factor Division, National Cancer Center Research Institute, Chuo-ku, Tokyo 104-0045, Japan

Submitted December 13, 2005; Revised April 25, 2006; Accepted May 1, 2006
Monitoring Editor: Richard Assoian

Crk-associated substrate (Cas) is a tyrosine-phosphorylated docking protein that is indispensable for the regulation of the actin cytoskeletal organization and cell migration in fibroblasts. The function of Cas in neurons, however, is poorly understood. Here we report that Cas is dominantly enriched in the brain, especially the cerebellum, of postnatal mice. During cerebellar development, Cas is highly tyrosine phosphorylated and is concentrated in the neurites and growth cones of granule cells. Cas coimmunoprecipitates with Src family protein tyrosine kinases, Crk, and cell adhesion molecules and colocalizes with these proteins in granule cells. The axon extension of granule cells is inhibited by either RNA interference knockdown of Cas or overexpression of the Cas mutant lacking the YDxP motifs, which are tyrosine phosphorylated and thereby interact with Crk. These findings demonstrate that Cas acts as a key scaffold that links the proteins associated with tyrosine phosphorylation signaling pathways to the granule cell axon elongation.

INTRODUCTION

Crk-associated substrate (Cas) docking protein was initially identified as a major phosphotyrosine-containing protein in fibroblasts transformed by *v-Src* or *v-Crk* oncogenes (Sakai *et al.*, 1994). It has an N-terminal Src homology 3 (SH3) domain, a substrate domain (SD) that consists of a cluster of tyrosine phosphorylation sites and a C-terminal Src-binding domain (SBD) that functions to directly bind the Src family protein tyrosine kinases (PTKs; Sakai *et al.*, 1994; Nakamoto *et al.*, 1996). In motile cells such as fibroblasts, Cas is tyrosine-phosphorylated by Src or Fak family PTKs after integrin stimulation, which induces Cas localization to focal adhesions. Tyrosine-phosphorylated Cas (YP-Cas) acts as a scaffold protein upstream of the Rho family small GTPase in focal adhesions (O'Neill *et al.*, 2000). Embryonic fibroblasts lacking the Cas gene exhibit impaired actin stress fiber bundling and cell motility, indicating that Cas is indispensable for actin cytoskeleton organization and cell migration (Honda *et al.*, 1998; Huang *et al.*, 2002). The function of Cas in neurons, however, is unknown.

Neurons extend neurites immediately after exiting from mitotic cycles. At the tip of the extending neurites, there are motile enlargements, growth cones that build the dynamic center for signaling of the mobility and direction of extending neurites. Filopodia and lamellipodia are two dynamic structures in the growth cone that rapidly extend and retract, providing the force to advance in response to extracellular cues. Filopodia are protrusions composed of bundled F-actin fibers, whereas lamellipodia are large fanlike structures composed of a cross-linked actin meshwork (Tanaka and Sabry, 1995; Luo, 2002). The signaling pathways from the surface to the actin cytoskeletal organization in growth cones are essential for neurite outgrowth (Dickson, 2001; Dent and Gertler, 2003; Pollard and Borisy, 2003). Protein tyrosine phosphorylation is the critical factor for the signaling cascades that control growth cone motility (Korey and Van Vactor, 2000).

Cerebellar granule cells are the most abundant cell population in the cerebellar circuit. Granule cells proliferate postnatally in the external granule layer (EGL). Postmitotic granule cells move into the inner half of the EGL (iEGL) where they begin to differentiate. While migrating further down the molecular layer (ML) to the internal granule layer (IGL), granule cells develop the characteristic morphologies of their axons, parallel fibers (Ono *et al.*, 1997). Granule cells settle in the IGL and develop their dendritic morphologies, forming synaptic glomerular rosettes with mossy fiber terminals and Golgi cell axon terminals. Src family PTKs such as Src, Fyn, Yes, Lyn, and Lck are highly expressed in the cerebellum, and their expression is developmentally regulated (Fults *et al.*, 1985; Cartwright *et al.*, 1988; Maness *et al.*, 1988; Sudol *et al.*, 1988, 1989; Zhao *et al.*, 1991; Chen *et al.*, 1996; Omri *et al.*, 1996). The PTK activity of Src in the developing cerebellum is ~6- to 10-fold that in fibroblasts (Cartwright *et al.*, 1988). High levels of Src, Fyn, and Yes are concentrated in the growth cones of cerebellar neurons (Maness *et al.*, 1988; Wu and Goldberg, 1993). Src family PTKs are implicated in the signaling pathways of cell adhesion molecule (CAM)-induced neurite outgrowth. Cultured cerebellar neurons prepared from mice lacking Fyn do not extend axons on neuronal cell adhesion molecule (NCAM)-

This article was published online ahead of print in *MBC in Press* (http://www.molbiolcell.org/cgi/doi/10.1091/mbc.E05-12-1122) on May 10, 2006.

[D] The online version of this article contains supplemental material at *MBC Online* (http://www.molbiolcell.org).

Address correspondence to: Teiichi Furuichi (tfuruichi@brain.riken.jp).

Abbreviations used: Cas, Crk associated substrate; YP-Cas, tyrosine phosphorylated Cas; SD, substrate domain; SBD, Src binding domain; PTK, protein tyrosine kinases; CAM, cell adhesion molecules; NCAM, neuronal cell adhesion molecule; EGL, external granule cell layer; ML, molecular layer; IGL, internal granule cell layer; PL, Purkinje cell layer; WM, white matter; EGFP, enhanced green fluorescent protein; GCP, growth cone particle.

coated culture matrix as rapidly as cells from wild-type littermates (Beggs *et al.*, 1994). Similarly, cerebellar granule cells from Src-deficient mutant mice show impaired neurite outgrowth on the neural adhesion molecule L1 (Ignelzi *et al.*, 1994). These results suggest that Src and Fyn have important roles in granule cell neurite extension. The signaling cascade from the CAMs and Src family PTKs to the cytoskeleton, however, remains to be clarified.

The present study demonstrates that among tissues of postnatally developing mice, Cas is most abundant in the brain, especially in the cerebellum. It is notable that YP-Cas peaked around the first postnatal week and was concentrated in the growth cone fractions. The Cas protein was immunocytochemically localized in the growth cones and neurites of granule cells. In the cerebellum, Cas coimmunoprecipitated with Src family PTKs, Crk, and CAM proteins N-cadherin and NCAM. Granule cell axon elongation was impaired by either RNA interference (RNAi) knockdown of Cas or overexpression of Cas mutants with deletion of the multiple tyrosine phosphorylation sites that confer the Crk-binding property. Our results suggest that YP-Cas acts as an important scaffold in the signaling of axon elongation of cerebellar neurons, linking extracellular signals to the cytoskeleton through tyrosine phosphorylation.

MATERIALS AND METHODS

Primary Dissociated Cerebellar Cell Culture

Cerebellar cells were prepared from postnatal day 0 (P0) ICR mouse cerebella as described previously (Shiraishi *et al.*, 1999). In brief, the cerebella from P0 mice were treated with 0.1% trypsin (Sigma Chemical, St. Louis, MO) and 0.05% DNase I (Roche Diagnostics, Indianapolis, IN) in Ca^{2+}-Mg^{2+}-free Hanks' balanced salt solution (HBSS), dissociated by repeated passage through a micropipette tip in Ca^{2+}-Mg^{2+}-free HBSS containing 0.05% DNase I and 12 mM $MgSO_4$, and then rinsed with the culture medium. Dispersed cells (4×10^5) were plated onto poly-L-lysine (Sigma)-coated glass coverslips (12-mm diameter; Matsunami, Tokyo, Japan) in serum-free defined medium: Eagle's medium supplemented with 1 mg/ml bovine serum albumin, 10 μg/ml insulin, 0.1 nM L-thyroxine, 0.1 mg/ml transferrin, 1 μg/ml aprotinin (all from Sigma), 30 nM selenium (Merck, Darmstadt, Germany), 0.25% (wt/vol) glucose, 2 mM glutamine, 2 mg/ml sodium bicarbonate, 0.1 mg/ml streptomycin (Meiji Seika KK, Tokyo, Japan), and 100 U/ml penicillin (Banyu Pharmaceutical, Tokyo, Japan). The cultures were maintained in a humidified atmosphere of 5% CO_2 in air at 37°C.

Primary Cerebellar Neuron Transfection and Axon Length Analysis

Cas mutants produced as described previously (Huang *et al.*, 2002) were constructed in a plasmid vector that contains the CAG promoter. Short interfering RNA (siRNA) of Cas was generated using the BLOCK-iT RNAi TOPO Transcription and BLOCK-iT Complete Dicer RNAi kits (Invitrogen, Carlsbad, CA) according to the manufacturer's instructions (Azuma *et al.*, 2005). siRNA of LacZ was generated using the same procedure as for Cas siRNA and was used as a negative control. Transfection of cerebellar neurons was performed soon after the neurons were dissociated using the Mouse Neuron Nucleofector kit and the Nucleofector device (Amaxa, Cologne, Germany; Liu *et al.*, 2003; Hama *et al.*, 2004). The transfection efficiency was 5%. The calcium phosphate method using a CellPhect Transfection Kit (Amersham Biosciences, Buckinghamshire, United Kingdom) was also used to transfect cerebellar neurons on day 1 in vitro (DIV1) in serum-free defined medium on poly-L-lysine–coated glass coverslips. The length of the longest axon was quantified in granule cells (marked by immunolabeling with antibody against Pax6) expressing the Cas mutant or siRNA. Axons were also confirmed by immunolabeling with antibody against Tau-1. Axons could be easily distinguished from dendrites because granule cells at DIV2 exhibit a representative morphology with a long single or bipolar axon with multiple short dendrites (Powell *et al.*, 1997). The percentage of granule cells with axons longer than 200 μm in each transfection case was quantified in at least 20 fields randomly selected from three independent experiments. Student's *t* test was used to compare results between the mutant and the control cells. $p < 0.05$ was considered significant.

RT-PCR Analysis

A series of first-strand cDNAs was produced by reverse-transcription (RT) from 20 ng of total cerebellar RNAs at the various developmental stages, using an oligo-dT primer. The cDNA sequence corresponding to the nucleotide positions 583-1182 (amino acids 175–394) of p130Cas was amplified using the primers 5′-ACATCTACCAAGTCCCTCCA-3′ (forward primer) and 5′-AGGCACGTCATACAGTGTTC-3′ (reverse primer). The cycling conditions were as follows: denaturing at 94°C for 3 min, amplification by 25 cycles of 94°C (15 s), 55°C (2 min), and 72°C (1 min), and extension at 72°C for 5 min. To analyze tissue distribution, total RNAs prepared from various tissues of P7 or P21 mice were used for RT-PCR. The RT-PCR of glyceraldehyde-3-phosphate dehydrogenase with primers 5′-GCCATCAACGACCCCTTCATTGAC-CTC-3′ (forward primer) and 5′-GCCATGTAGGCCATGAGGTCCACCAC-3′ (reverse primer) were used as an internal control.

In Situ Hybridization

In situ hybridization brain histochemistry was basically performed as described previously(Shiraishi *et al.*, 1999). The cDNA sequence corresponding to nucleotide positions 583-1182 (amino acids 175–394) of the p130Cas cDNA was used as a template to prepare the digoxigenin-labeled antisense riboprobes using a digoxigenin-dUTP labeling kit (Roche Diagnostics). Paraffin sections of mouse brain (10 μm thick) were fixed in 4% paraformaldehyde for 5 min, washed twice in phosphate-buffered saline (PBS), and treated with freshly prepared 10 μg/ml proteinase K (Invitrogen) at room temperature. After acetylation, the sections were subjected to digoxigenin-based hybridization procedures. Briefly, the sections were incubated in a hybridization buffer containing 0.2 μg/ml digoxigenin-labeled riboprobes at 60°C overnight in a humid chamber. The hybridized sections were washed by successive immersion in 1× SSC (150 mM NaCl and 15 mM sodium citrate, pH 7.0, 60°C, 10 min, twice), 2× SSC (37°C, 10 min), 2× SSC containing 20 μg/ml RNase A (37°C, 30 min), 2× SSC (37°C, 10 min), and 0.2× SSC (60°C, 30 min, twice). The hybridization signals were detected using the digoxigenin detection kit (Roche Diagnostics).

Immunoprecipitation and Immunoblotting

Protein extraction and Western blotting analysis were performed as described previously (Huang *et al.*, 2002). Briefly, mouse cerebella or cerebra were lysed in 1% Triton X-100 buffer (50 mM HEPES, 150 mM NaCl, 10% glycerol, 1% Triton X-100, 1.5 mM $MgCl_2$, 1 mM EGTA, 100 mM NaF, 1 mM Na_3VO_4, 10 μg/ml aprotinin, 10 μg/ml leupeptin, and 1 mM phenylmethylsulfonyl fluoride). Aliquots of protein lysates were separated by SDS-PAGE and probed with diluted antibodies. For immunoprecipitation, protein (500 μg) was mixed with 1 μg primary antibody and incubated for 1 h on ice. The mixtures were rotated with protein A- or protein G-Sepharose (Amersham) for 1 h at 4°C. The Sepharose were washed four times with 1% Triton X-100 buffer and boiled in sample buffer before being subjected to SDS-PAGE analysis.

Antibodies

Antibodies against mouse Cas were used as described previously (Sakai *et al.*, 1994). A phospho-specific polyclonal antibody (αCas-pYDxP) that specifically recognizes YP-Cas was generated by immunizing rabbits with a synthetic peptide, CAEDV(pY)DVP (a.a. 456–463), which is representative of the repetitive tyrosine-containing motifs in the Cas SD, after being conjugated with thyroglobulin (Miyake *et al.*, 2005). Antibodies against Src family tyrosine kinases, N-cadherin, L1, β-integrin, NCAM140/180, hemagglutinin (HA), and Crk were from BD Bioscience (Franklin Lakes, NJ). The antibodies against Fyn (Fyn3), c-Src (N-16), NCAM120, and JNK1 were from Santa Cruz Biotechnologies (Santa Cruz, CA). The antibody anti-GAP43 was from Innogenetics (Alpharetta, GA). The antibodies against phosphotyrosine 4G10 was from Upstate Biotechnology (Waltham, MA), antibodies against Map2 (AP20) and calbindin were from Sigma, the antibody against Pax-6 was from Covance (Princeton, NJ), and the antibody against tau-1 was from Chemicon International (Temecula, CA).

Subcellular Fractionation and Isolation of Growth Cone Particles

P7 and P21 mouse cerebella were homogenized in the homogenization buffer (0.32 M sucrose, 5 mM Tris-HCl, 1 mM EGTA, 1 mM DTT, 1 mM pepstatin A, 1 mM leupeptin, and 1 mM Na_3VO_4). The protein homogenates were centrifuged at 1000 × *g* for 10 min. The pellet was lysed in 1% Triton X-100 buffer (PPt1). The supernatant was recentrifuged at 105,000 × *g* for 1 h. The pellet was lysed in 1% Triton X-100 buffer (PPt2 + 3), and the supernatant was used as Sup3. Growth cone particles (GCP) were prepared essentially as described previously (Pfenninger *et al.*, 1983; Helmke *et al.*, 1998). P7 mouse cerebella were homogenized in ~8 volumes of 0.32 M sucrose containing 1 mM $MgCl_2$ and 1 mM TES buffer, pH 7.3. The homogenate was centrifuged at 2000 rpm for 10 min (pellet, PPt1), and the resulting low-speed supernatant (cytosol) was loaded onto a discontinuous density gradient with steps of 0.75 and 1 M sucrose in the same buffer. The gradients were spun to equilibrium at 28,000 rpm for 1 h in a swing rotor SW-28 (Beckman Coulter, Fullerton, CA). The fraction at the 0.32/0.75 M sucrose interface containing the GCPs was collected. This fraction was diluted 3- to 4-fold with 0.32 M sucrose, and GCPs were pelleted at 40,000 rpm for 30 min (TLA-100, Beckman) and extracted with 1% Triton X-100 buffer for 30 min at 4°C (GCP).

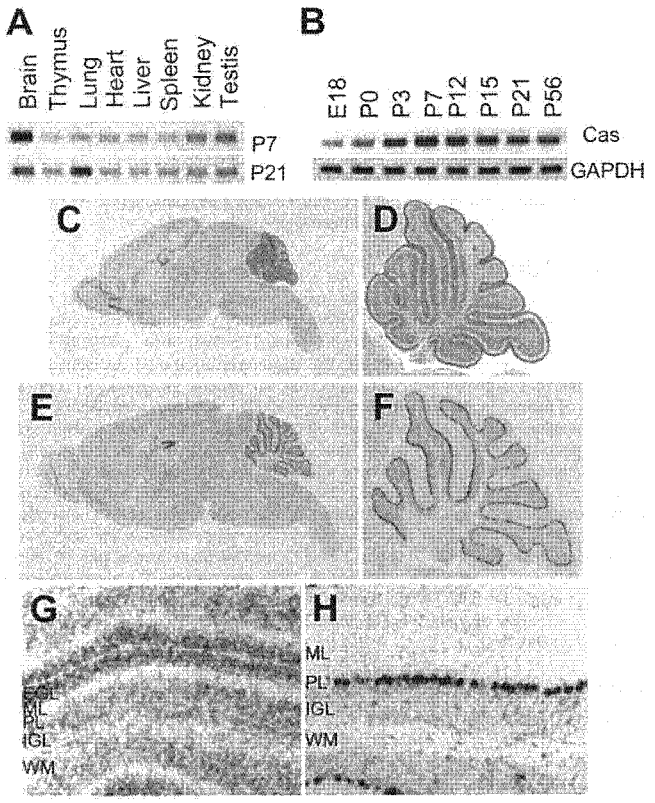

Figure 1. Expression of Cas mRNA in developing mouse cerebella. (A) Semiquantitative RT-PCR analysis of Cas mRNA expression in P7 or P21 mouse tissue. (B) RT-PCR analysis of Cas mRNA expression in postnatal cerebella at six different postnatal stages. RT-PCR for GAPDH was used as an internal control. (C–H) In situ hybridization analysis of Cas distribution in the P7 (C, D, and G) and P21 (E, F, and H) mouse brains. C, P7 brain; D, P7 cerebellum; E, P21 brain; F, P21 cerebellum; G, P7 cerebellar cortex; H, P21 cerebellar cortex. EGL, external granule cell layer; ML, molecular layer; IGL, internal granule cell layer; PL, Purkinje cell layer; WM, white matter.

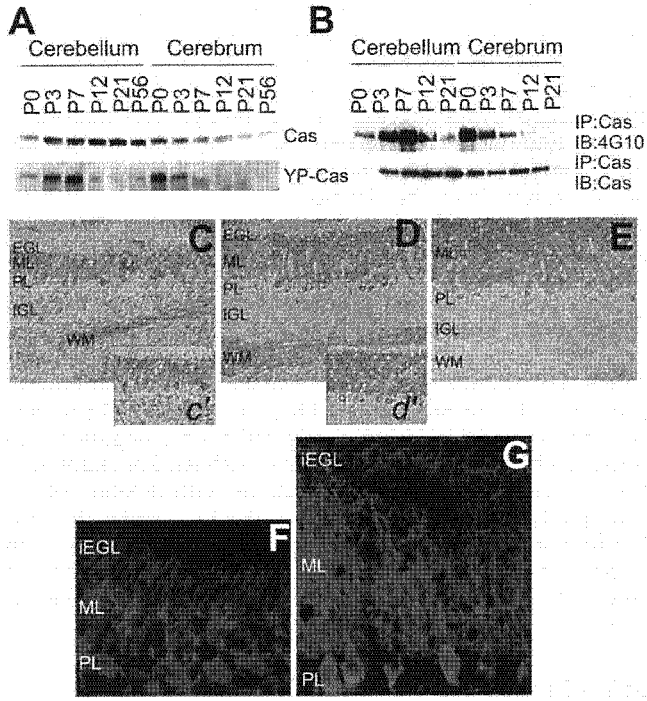

Figure 2. Expression and tyrosine phosphorylation of Cas protein in developing mouse cerebella. (A) Immunoblotting of Cas and YP-Cas in the postnatal cerebella. Approximately equal amounts of protein lysates from six different postnatal stages (P0, P3, P7, P12, P21, and P56) were subjected to immunoblotting analysis by an antibody against Cas or YP-Cas. (B) Immunoprecipitation with the Cas antibody followed by immunoblotting with the phospho-tyrosine antibody 4G10. (C–E) Immunohistochemical staining of Cas in the P7 (C and c'), P12 (D and d'), and P21 (E) mouse cerebella sections. (F and G) Immunohistochemical analysis of YP-Cas detected by the specific antibody (red) in P7 (F) and P12 (G) mouse cerebella. Purkinje cells were immunostained with anti-calbindin antibody (green). iEGL, the inner half of EGL.

Immunohistochemistry and Fluorescent Microscopy

The cells were fixed with 4% paraformaldehyde for 1 h, washed three times with PBS, and then permeabilized with 0.2% Triton X-100/PBS for 5 min before incubation with 5% normal goat serum in PBS (−). For native tissues, ICR mice were transcardically perfused with 4% paraformaldehyde in PBS (−), and the dissected brains were immersed for 2 h in the same fixative buffer and cryosectioned (20 μm thick). For immunoreaction, fixed cultured cells or brain sections were preincubated with 5% normal goat serum in PBS (−) for 1 h and then incubated with primary antibody (anti-Cas, 1 μg/ml), for 1 h at room temperature. After washing with PBS (−), the samples were incubated with Alexa-conjugated secondary antibody (Invitrogen). Immunofluorescence was observed using a Zeiss (Oberkochen, Germany) Meta-510 confocal laser microscope. Conventional immunostaining reaction was also performed using a diaminobenzidine and horseradish peroxidase–conjugated secondary antibody.

RESULTS

Cas mRNA Is Abundantly Expressed in Developing Mouse Cerebella

To examine the functional role of Cas in the mouse CNS, we first analyzed the expression of Cas mRNA in mice at P7 and P21 using RT-PCR technique. Of the eight tested tissues of P7 mice, the expression level of Cas mRNA was highest in the brain (Figure 1A). Cas mRNA was also expressed abundantly in P21 brain. In situ hybridization analysis revealed strong Cas mRNA labeling in the cerebellum, hippocampus, and olfactory bulb at P7 (Figure 1C) and P21 (Figure 1E). The cerebellum was the predominant region with Cas mRNA expression at P7 (Figure 1D) and P21 (Figure 1F). During postnatal cerebellar development, Cas mRNA expression was up-regulated, with the peak occurring from P7 to P12 (Figure 1B). In the P7 cerebella, Cas mRNA was primarily concentrated in the EGL, and was also present in the IGL, Purkinje cell layer (PL), and white matter (WM; Figure 1G). In P21 cerebella, on the other hand, it was predominantly localized in the PL and present in only low levels in the IGL and WM (Figure 1H). These results suggested that Cas has a functional role(s) in cerebellar development.

Cas Protein Is Highly Tyrosine-phosphorylated during Cerebellar Development

We investigated the expression and tyrosine phosphorylation of Cas protein in developing mouse brains at six different postnatal stages (P0, P3, P7, P12, P21, and P56) by immunoblotting analysis (Figure 2A). The tyrosine-phosphorylated Cas (YP-Cas) was immunodetected by an antibody that recognizes the tyrosine-phosphorylated YDxP motifs of Cas (Miyake *et al.*, 2005). In the cerebella, Cas protein expression was up-regulated to a peak level at around P21 and then slightly down-regulated, which almost paralleled the mRNA expression profile (Figure 1B). In contrast to this developmental profile of Cas expression, YP-Cas

rapidly increased after birth to reach a peak level at P7 and then sharply decreased. This steep increase of YP-Cas within the first postnatal week was also confirmed by an immunoprecipitation assay with the anti-Cas antibody followed by immunoblotting with the anti-phospho-tyrosine antibody 4G10 (Figure 2B). In the cerebra, on the other hand, both Cas and YP-Cas proteins were most abundant at P0 and then markedly decreased (Figure 2, A and B).

We then immunohistochemically analyzed the cellular distribution of Cas protein in the developing cerebella (Figure 2, C–E). In P7 cerebella, there was intense Cas immunolabeling in the ML and PL and weak immunolabeling in the EGL, IGL, and WM (Figure 2C). In P12 cerebella, there was high density labeling in the ML, PL, and WM and low density labeling in the IGL (Figure 2D). In P21 cerebella, there was strong Cas staining in the ML and PL and weak staining in the WM (Figure 2E). On the other hand, YP-Cas had characteristic cellular distribution patterns in the developing cerebella (Figure 2, F and G). Intense YP-Cas immunolabeling was distributed primarily in the iEGL and ML at P7 (F) and in the iEGL at P12 (G), and moderate labeling was observed in the WM at P7 and P12 (unpublished data). In the P12 ML, there was weak YP-Cas immunolabeling around the growing dendrites of Purkinje cells, which were coimmunostained for calbindin (a Purkinje cell marker; Figure 2G). At P21, there was very weak immunostaining in the ML and IGL (unpublished data). These data indicate that Cas is highly tyrosine-phosphorylated in postmitotic premigratory granule cells within the iEGL, in outgrowing Purkinje cell dendrites within the ML, and in the WM (probably in Purkinje cell axons), at the first and second postnatal stages.

Cas Is Enriched in the Growth Cones of Developing Cerebellar Neurons

We performed subcellular fractionation of Cas protein from P7 and P21 mouse cerebella. Cas immunoreactivity was recovered in the precipitation fractions, PPt1 (nuclei and cytoskeleton fractions) and PPt2 + 3 (membrane fraction containing mitochondria and microsomes), and the supernatant fraction Sup3 (cytosolic; Figure 3A, bottom). On the other hand, YP-Cas immunoreactivity was enriched in the precipitation fractions: in the PPt1 and PPt2 + 3 at P7 and in the PPt2 + 3 at P21 (Figure 3A, top). Moreover, YP-Cas was concentrated in the GCP fraction prepared from P7 cerebella, in which a growth cone marker, growth-associated protein 43 (GAP43), was recovered (Figure 3B).

We next analyzed the subcellular localization of Cas protein in cultured cerebellar neurons (Figure 3, C–I). Cas was detected in axons of granule cells at DIV1, and was largely concentrated in their fanlike tips, growth cones (Figure 3, C–L). Although the fine structure of granule cell growth cones was difficult to observe because of their thin and tiny morphology, Cas was localized in both the central and peripheral domains (Figure 3, F–I), and colocalized with actin bundles (Figure 3, J–L'). In cultured Purkinje cells (DIV14), Cas immunoreactivity was observed in the tips of the dendritic arbors as well as in their dendrites, axons, and soma (unpublished data). These data indicate that Cas is subcellularly localized in outgrowing neurites and growth cones of cerebellar neurons. The subcellular fractionation analysis implied that Cas in growth cones is highly tyrosine-phosphorylated.

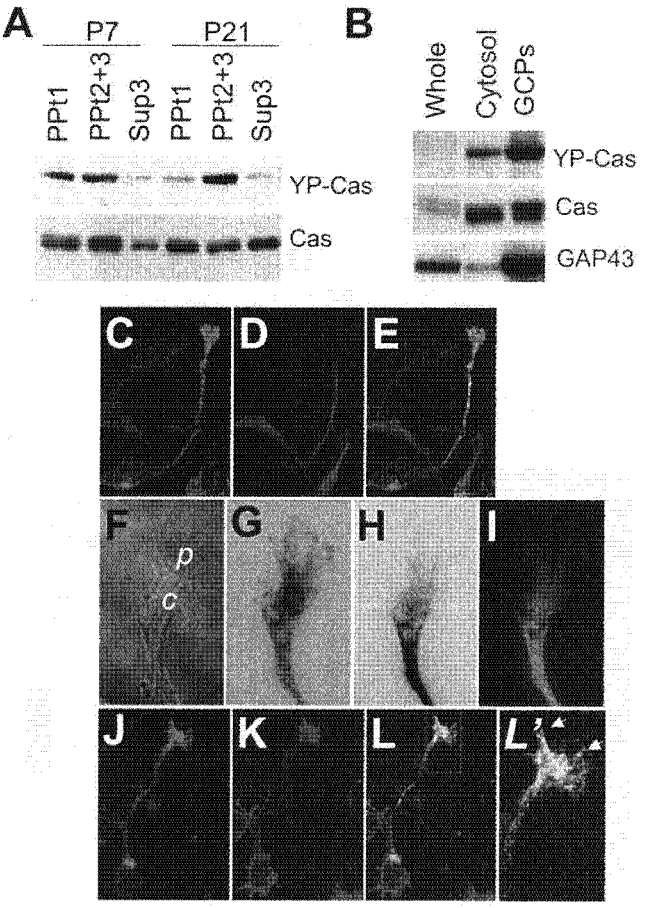

Figure 3. Cas is enriched in the growth cones of cerebellar granule cells. (A) Immunoblotting of Cas in subcellular protein fractions from P7 and P21 mouse cerebella. (B) Immunoblotting of Cas and YP-Cas in growth cone fractions from P7 mouse cerebella. Equal amounts of proteins were loaded in each lane and immunoblotted with antibodies against YP-Cas, Cas, and GAP43 (as a control of growth cone proteins). (C–E) Confocal images of Cas (C) and Map2 (D) in the granule cells (DIV1). (E) Merged image of C and D. (F–I) Phase-contrast images (F) of Cas (G) and Map2 (H) in the granule cell growth cones. (I) Merged image of G and H. (J–L'), Immunostaining of Cas (J) and F-actin (by phalloidin staining; K) in granule cells. (L) Merged image of J and K. (L') Magnified views of the growth cones. Arrows indicate colocalization of Cas and F-actin.

RNAi Knockdown of Cas Inhibits Axon Extension of Granule Cells

We examined whether interference of the endogenous Cas by RNAi affects granule cell axon extension (Figure 4A). The effectiveness of siRNAs was first evaluated in DLD-1 cells (human colon tumor cells), in which more than 90% of Cas protein expression was knocked down within 72 h after transfection (Supplementary Figure 1A). Then, the siRNA efficiency was confirmed by cotransfection of CasFL and Cas siRNA in cerebellar primary cultures (Supplementary Figure 1, B and C). Because of the transfection ratio and the difficulty in quantifying the Cas expression level changes in the primary culture by immunoblotting, the number of cells expressing the exogenous CasFL construct carrying the HA epitope in each observation field was quantified by HA immunostaining. HA-positive cells were decreased by cotransfection of Cas siRNA (~3 in each field), in comparison with that of the control LacZ (*Escherichia coli* β-galactosidase

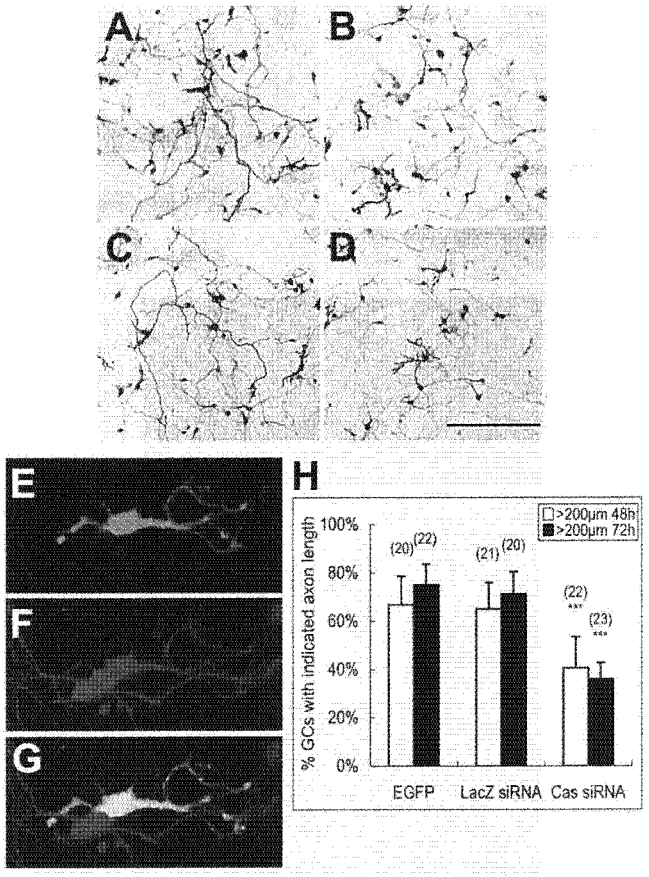

Figure 4. RNAi knockdown of Cas impairs axon extension of cerebellar granule cells. (A–D) Confocal images of cerebellar granule cells transfected with Cas siRNA or LacZ siRNA. Cerebellar granule cells were cotransfected soon after cell dissociation by either Cas siRNA or LacZ siRNA with pCAG-EGFP. Cells were fixed and observed 48 or 72 h after the transfection. (A) LacZ siRNA 48 h; (B) Cas siRNA 48 h; (C) LacZ siRNA 72 h; (D) Cas siRNA 72 h. Scale bar, 200 μm. (E–G) Granule cells (stained by anti-Pax6 antibody; F) with multiple short axons observed in Cas siRNA transfection (E). (H) Percentage of cells with axons longer than 200 μm within each observation field 48 or 72 h after transfection. Data are presented as mean ± SEM. Values in the parentheses above the column indicate the number of observation fields from at least three independent experiments. ***$p < 0.001$, compared with the EGFP control (*t* test).

gene) siRNA (~10 in each field), demonstrating that Cas siRNA specifically knocked down Cas proteins in granule cells.

The knockdown effect of Cas siRNA on neurite extension of granule cells was analyzed by counting cells with an axon length of more than 200 μm cotransfected with Cas siRNA and enhanced green fluorescent protein (EGFP) in comparison with controls. The control granule cells, which were cotransfected with LacZ siRNA and EGFP, exhibited an almost normal neurite pattern with long axons at 48 and 72 h (Figure 4, A and C, respectively) after transfection. In contrast, cells cotransfected with the Cas siRNA and EGFP had an impaired axon pattern at 48 and 72 h (Figure 4, B and D, respectively) after transfection. Pax6 (a granule cell marker)-positive cells coexpressing Cas siRNA and EGFP formed a complex neurite pattern with short, branched axons (Figure 4, E–G), indicating that Cas knockdown affected the granule cells. Long axons (>200 μm) extended from 65 and 72% LacZ siRNA-expressing granule cells at 48 and 72 h after transfection, respectively (Figure 4H). These ratios were almost comparable with those in cells expressing EGFP alone. The number of long axons (>200 μm) was significantly reduced in Cas siRNA-expressing granule cells to 40 and 35% at 48 and 72 h after transfection, respectively (Figure 4H). This Cas siRNA knockdown effect was observed even in granule cells overexpressing exogenous CasFL protein (Supplementary Figure 1D). Therefore, our data suggest that Cas is related to granule cell axon elongation.

Deletions of the YDxP Motifs or the Cas Substrate Domain Impairs Axon Elongation of Granule Cells

Cas consists of three major protein-protein interaction domains (Figure 5A): the N-terminal SH3 domain (binds to the PxxP motif of Fak, Pyk2, PTP1B, etc.), the SD (consists of a cluster of YxxP motifs that are tyrosine-phosphorylated by PTKs, leading to binding to Crk, Nck, SHIP-2, etc.), and SBD (containing motifs RPLPSPP [a.a.733–739] and YDYV [a.a.762–765], which bind to Src family PTKs; Sakai *et al.*, 1994). To assess the structure and function relationship of Cas protein in granule cell development, we constructed four Cas mutants: three deletion mutants lacking the SH3 (ΔSH3), SD (ΔSD), or only YDxP motifs within the SD (ΔYDxP), and a substitution mutant of the RPLPSPP and YDYV motifs within the SBD to RLGSSPP and FDYV, respectively (mSBD; Figure 5A). Either the full-length Cas (CasFL) or mutant Cas was coexpressed with the EGFP vector in cultured granule cells by transfection (Figure 5B). Expressed EGFP fluorescence was generally widespread over the soma and neurites of granule cells. Granule cells transfected with the CasFL, ΔSH3, or mSBD exhibited a representative morphology with single or bipolar long extending axons at this stage (DIV2; Ono *et al.*, 1997; Powell *et al.*, 1997), whereas cells transfected with the ΔSD or ΔYDxP tended to have significantly shorter, and sometimes branching, axons (Figure 5B), similar to that observed in Cas knockdown cells by Cas siRNA (Figure 4, E–H). These short axons were immunopositive for Tau-1 (unpublished data). The average length of the longest axon, in cells expressing CasFL, ΔSH3, or mSBD was nearly 250 μm, whereas that of cells expressing the ΔSD (~58 μm) or ΔYDxP (~76 μm) was very short (Figure 5C). Long axons (>200 μm) extended from more than 70% of CasFL, ΔSH3, mSBD, and EGFP-expressing cells, whereas they were observed in fewer than 40% of ΔSD or ΔYDxP-expressing cells (Figure 5D). These results suggest that the SD containing the YDxP motifs is involved in the axon elongation of granule cells and that the ΔSD and ΔYDxP act as dominant negatives to endogenous Cas in this process. The F-actins in the granule cells overexpressing Cas mutants were labeled (Supplementary Figure 4); however, there were no significant differences in the quantity of F-actins in the growth cones of cells expressing ΔYDxP and other mutants.

Cas Is the Substrate of Src Family Tyrosine Kinases in the Developing Mouse Cerebella

In fibroblasts, Cas binds to both Src and Fak family PTKs and is consequently phosphorylated by them (Nakamoto *et al.*, 1996; Cary *et al.*, 1998). To elucidate the molecular basis of Cas tyrosine phosphorylation during mouse cerebellar development, we investigated the association of Cas with nine PTKs belonging to the Src or Fak family (Figure 6). Seven Src family (Src, Fyn, Lyn, Yes, Hck, Lck, and Zap70) and the two Fak family (Fak and Pyk2) PTKs tested were expressed in the mouse cerebella (unpublished data). Only Src family PTKs, however, coimmunoprecipitated with Cas in P7 cerebellar extracts (Figure 6A), suggesting that the Src

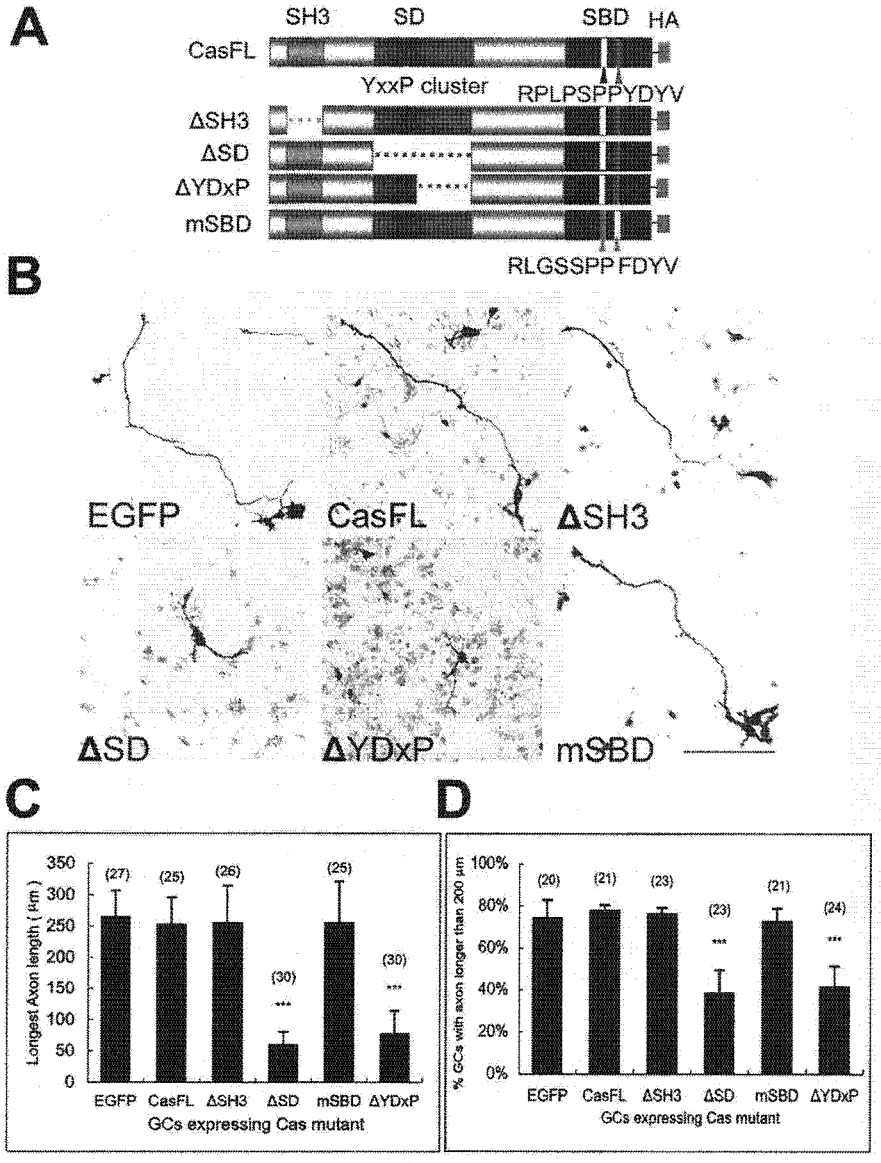

Figure 5. Overexpression of the Cas mutant lacking Crk binding ability inhibits axon elongation of granule cells. (A) Cas mutants with domain deletion or mutation. ΔSH3, deletion of the SH3 domain; ΔSD deletion of a cluster of tyrosine phosphorylation sites; ΔYDxP, deletion of YDxP motifs; mSBD, double mutations RLGSSPP and FDYV at the Src binding domain. (B) Confocal images of cerebellar granule cells expressing Cas mutants. Cerebellar granule cells were double-transfected by electroporation with a Cas mutant with an EGFP vector soon after dissociation of cerebellar cells. The cells were stained with the antibody against HA 48 h after plating. Bar, 100 μm. (C) Average length of the axons in the EGFP and Cas mutants coexpressing cells. (D) Percentage of transfected cells with axon length more than 200 μm. Cerebellar granule cells (DIV1) were transfected with Cas mutants using the calcium phosphate method. Cells were fixed, stained with the antibody against HA, and observed at DIV2. Data are indicated as mean ± SEM. Values in the parentheses above the column indicate the number of the transfected cells from at least three independent experiments. ***$p < 0.001$, compared with the EGFP control (*t* test).

family, but not the Fak family, associates with Cas in the mouse cerebella at the early stage. This result was confirmed by in vitro experiments using a Src family PTK inhibitor PP2. In contrast to the ineffective structural analog PP3, PP2 inhibited the tyrosine phosphorylation of Cas in cultured cerebellar cells (Figure 6B). YP-Cas was reduced to an almost undetectable level by treatment with 25 μM PP2, indicating that Src family PTKs are responsible for the tyrosine phosphorylation of Cas in these cells. Src and Fyn were enriched in the GCP fraction of the P7 cerebella (Supplementary Figure 2A), and their tyrosine phosphorylation levels were high in the P3–P7 cerebella (Supplementary Figure 2B). Immunocytochemical analysis of cultured granule cells (DIV1) revealed colocalization of Cas with Src and Fyn in the growth cones (Figure 6C). In addition, Cas was colocalized with Src, Fyn, or Yes in the cerebellar cortex at P12 (Supplementary Figure 2C). Moreover, there was a punctate accumulation pattern of the mSBD along the neurites (Supplementary Figure 3A). There were similar phenotypes in cells expressing ΔSBD (unpublished data). Although the underlying mechanism of punctuate distribution on neurites is unclear, it might be related to tyrosine phosphorylation, because exogenously expressed CasFL had a similar punctate accumulation pattern when PTK activity was inhibited with PP2 for 1 h (Supplementary Figure 3B).

Developmental Stage-specific Interaction of the Tyrosine-phosphorylated Cas with Adaptor Protein Crk in the Mouse Cerebellum

Crk is an adaptor protein that regulates actin cytoskeleton organization and cell migration (Klemke *et al.*, 1998). CrkII directly binds with YP-Cas in PC12 cells stimulated with nerve growth factor (Ribon and Saltiel, 1996). Our previous study indicated that YDxP motifs within the SD domain of Cas are involved in binding to CrkII in fibroblasts (Zhou *et al.*, 1993; Huang *et al.*, 2002). We examined whether there is an interaction between Cas and Crk in developing mouse cerebella (Figure 7, A and B). Crk protein was almost constantly expressed throughout cerebellar development (Figure 7A). Cas protein, however, was more efficiently coimmunoprecipitated with anti-Crk antibody from cerebellar extracts at P7 than from those at other stages tested (Figure 7B, top). In addition, the coimmunoprecipitated Cas was tyrosine phosphorylated (Figure 7B, middle). This P7 stage,

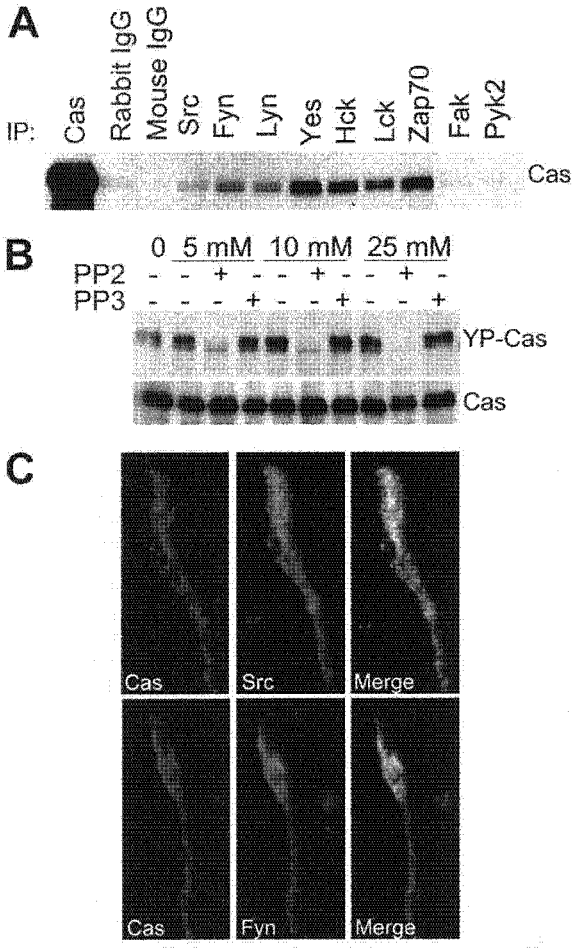

Figure 6. Cas is a substrate of Src family tyrosine kinases in the developing mouse cerebella. (A) Coimmunoprecipitation of Cas with the Src family PTKs in the mouse cerebella. An equal quantity of protein lysates from P7 cerebella was first immunoprecipitated by Src, Fyn, Yes, Lyn, Hck, Lck, Zap70, Fak, or Pyk2 antibodies and then immunoblotted by the Cas antibody. (B) Src family PTK inhibitor PP2 inhibited tyrosine phosphorylation of Cas in cerebellar neurons. Primary cultured cerebellar neurons were treated with dimethyl sulfoxide, PP2, or a noninhibitory analog, PP3, at the indicated concentrations for 20 min, and the cell lysates were immunoblotted for YP-Cas. The same membrane was reblotted to indicate the quantity of Cas in each lane. (C) Cas (red) colocalizes with Src or Fyn (green) in the growth cones of cultured cerebellar granule cells. Cerebellar granule cells were fixed at DIV1, stained, and imaged using confocal microscopy.

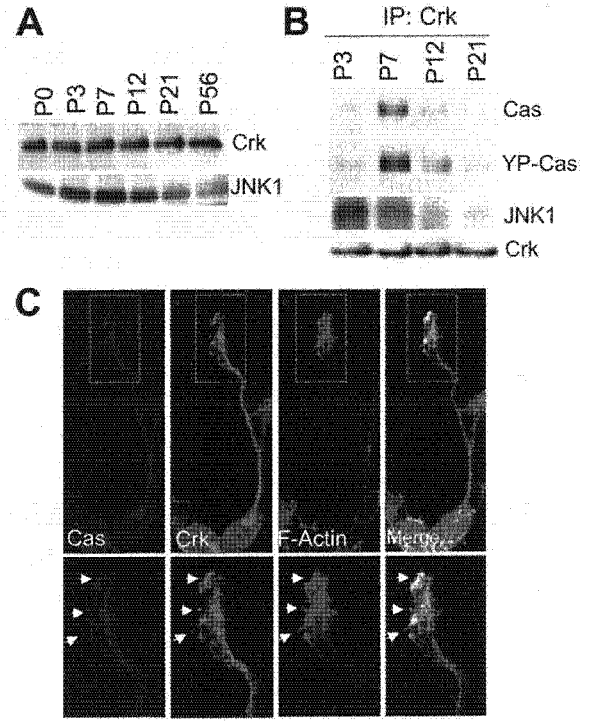

Figure 7. YP-Cas forms a complex with Crk-JNK1 in P7 mouse cerebella. (A) Immunoblotting of Crk and JNK1 protein in the mouse cerebella at different development stages. (B) Coimmunoprecipitation of Crk with Cas and JNK1 in developing mouse cerebella. An equal quantity of cerebella protein lysates from P3, P7, P12, and P21 mice were immunoprecipitated with the anti-Crk antibody and then immunoblotted with the antibody against Cas, YP-Cas, or JNK1. (C) Colocalization of Cas (blue), Crk (green), and F-actin (red, phalloidin staining) in the growth cones of cultured cerebellar granule cells (DIV1). Arrows indicate the colocalized structure.

in which there is a tight interaction between Cas and Crk, was consistent with the peak stage for tyrosine phosphorylation of Cas (Figure 2A). Moreover, both Cas and Crk immunolabels were codistributed in growth cones and neurites of cultured granule cells and were colocalized with actin bundles at the peripheral and central domains of growth cones (Figure 7C).

Because there is a direct interaction between CrkII and JNK1 (c-Jun N-terminal kinase 1; Girardin and Yaniv, 2001), we next investigated the Crk-JNK1 association. JNK1 expression was up-regulated with a peak at P7 and then down-regulated during mouse cerebellar development (Figure 7A). In immunoprecipitates with anti-Crk antibody, JNK1 was abundant in the early stages (P3–P7; Figure 7B). Taken together, these results suggest that the YP-Cas-Crk-JNK1 protein interaction is involved in the signaling pathway regulating actin organization of growth cones in granule cells.

Association of Cas with N-Cadherin and NCAM in the Developing Mouse Cerebellum

There are three major classes of CAMs in the nervous system: integrin, cadherin, and the IgG superfamily of CAM (IgCAM), which serve as plasma membrane sensors for extracellular cues, leading to the activation of intracellular signaling events related to the cytoskeleton (Walsh and Doherty, 1997). Cas is tyrosine-phosphorylated by Fak or Src family PTKs after integrin stimulation (O'Neill *et al.*, 2000). Therefore, we examined whether Cas is associated with CAMs in the mouse cerebella. Anti-Cas antibody coimmunoprecipitated with N-cadherin, NCAM, and L1, but not β-integrin, from P7 cerebellar extracts (Supplementary Figure 2D). The specific antibody for N-cadherin and NCAM coimmunoprecipitated with Cas protein from cerebellar extracts in the early developmental stage (Figure 8A). N-cadherin and NCAM140/180 mRNA were expressed in the EGL and IGL in postnatal mouse cerebella at P7 (Supplementary Figure 5), which coincides with the expression of Cas mRNA (Figure 1). Both N-cadherin and NCAM protein were enriched in the GCP fraction of P7 cerebella (Supplementary Figure 2A). Moreover, N-cadherin and NCAM colocalized with Cas in the growth cones and neurites of cultured granule cells (Figure 8B). Taken together, our data suggest that

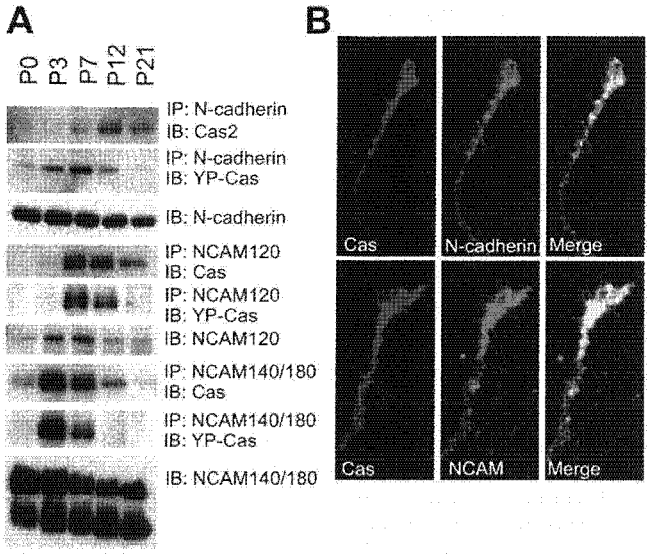

Figure 8. Cas and YP-Cas are developmentally associated with N-cadherin, NCAM120, or NCAM140/180 in mouse cerebella. (A) Cas and YP-Cas were coimmunoprecipitated with N-cadherin and NCAM in postnatal developing mouse cerebella. Equal amounts of protein lysate from the P0, P3, P7, P12, and P21 mouse cerebella were immunoprecipitated by antibodies against N-cadherin, NCAM120, or NCAM140/180. The immunoprecipitants were immunoblotted by the antibody against Cas. The same immunoprecipated protein blots were reused for immunoreaction with the antibody against YP-Cas. (B) Confocal images of colocalization of Cas (Red) with N-cadherin and NCAM140/180 (green) in the growth cones of cultured cerebellar granule cells (DIV1).

N-cadherin and NCAM interact with the Cas-mediated signaling complex and act as a cell surface signaling complex in granule cell neuritogenesis.

DISCUSSION

Cas acts as an indispensable scaffold for the signaling proteins involved in tyrosine phosphorylation–coupled actin cytoskeleton reorganization pathways and regulates cell morphology and migration in fibroblasts (Honda *et al.*, 1998; Huang *et al.*, 2002). The function of Cas in the nervous system, however, is unclear. Cas-deficient mice are embryonic lethal at 11.5–12.5 d after coitum because of impaired heart development (Honda *et al.*, 1998), making it difficult to investigate its role in the brain, which functionally develops later. The present findings demonstrate the functional importance of Cas as a signaling interface among the proteins involved in axon elongation of cerebellar granule cells during postnatal development.

The neural circuitry of the cerebellum develops through a coordinated program of neuronal migration, neurite outgrowth, and synaptic interconnections (Hatten and Heintz, 1995). To accomplish this circuit development, both granule cells and Purkinje cells undergo drastic morphological changes, in which actin cytoskeletal reorganization is very active (Ono *et al.*, 1997). The results of the present study demonstrated that both Cas mRNA and protein predominate in the cerebellum during this postnatal period in mice. Cas is enriched in the neurites and growth cones of developing granule cells and Purkinje cells. The specific binding of Cas to Src PTKs and consequent tyrosine phosphorylation, by which Cas acquires the critical ability to bind with downstream signaling proteins, peak in the early postnatal stage. This developmental profile of YP-Cas apparently coincides with the time window during which neurite extension of the granule cells and Purkinje cells are more active. In addition, YP-Cas is largely distributed around the iEGL, where postmitotic granule cells start to differentiate by axonal extension and migration, and the ends of Purkinje cell dendrites are actively sprouting. These results indicate that tyrosine phosphorylation of Cas is closely associated with the postnatal development of cerebellar neurons.

In fibroblasts, Cas interacts with Fak family PTKs through the N-terminal SH3 domain and also directly binds to Src family PTKs via the C-terminal SBD, which contains the YDYV and RPLPSPP motifs (Sakai *et al.*, 1994; Ruest *et al.*, 2001), resulting in the tyrosine-phosphorylation of Cas, the production of YP-Cas. Src family PTKs are highly expressed in the cerebellum and their expression and activity is developmentally regulated (Fults *et al.*, 1985; Cartwright *et al.*, 1988; Maness *et al.*, 1988; Sudol *et al.*, 1988, 1989; Chen *et al.*, 1996; Omri *et al.*, 1996). A previous study indicated that Fak has important roles in axon extension and polarization of cerebellar Purkinje cells (Rico *et al.*, 2004). There are no reports, however, of a role for Fak in cerebellar granule cell development. Our study demonstrated that Cas has no tight association with Fak and Pyk2 compared with Src family PTKs in early postnatal developing cerebella. Cas associates with Src family PTKs in developing mouse cerebella and colocalizes with Src and Fyn in the growth cones of granule cells. Moreover, the Src family PTK inhibitor PP2 almost completely blocks the tyrosine phosphorylation of Cas in in vitro cerebellar cell cultures. These findings support the idea that Src, but not Fak, family PTKs are responsible for the tyrosine phosphorylation of Cas in cerebellar neurons.

Cas is constitutively tyrosine-phosphorylated after binding to the Src family PTKs, and the major tyrosine phosphorylation sites are the SD, including four YQxP motifs and nine YDxP motifs in fibroblasts (Pellicena and Miller, 2001; Ruest *et al.*, 2001). We previously reported that Cas null fibroblasts have defective actin stress fiber organization and that the ΔYDxP Cas mutant fails to restore the actin stress fiber organization (Huang *et al.*, 2002). In the present study, knockdown of Cas protein expression with the Cas siRNA impaired axonal growth, and dominant-negative effects of Cas mutants, ΔSD and ΔYDxP, in axon elongation were also observed. Granule cells expressing exogenous ΔSD or ΔYDxP have abnormally truncated axonal protrusions, whereas no abnormal axon elongation was observed in cells expressing the other mutants ΔSH3 and mSBD, indicating the importance of the interaction of Cas with the SD-binding proteins for axon extension of granule cells. On the other hand, the overexpressed mSBD mutant tended to distribute in a punctate pattern in the dendrites and soma (Supplementary Figure 3), suggesting that a defect in the binding of Cas to Src family PTKs affects the subcellular distribution of Cas proteins. Loss of the dominant negative effect of mSBD on axon extension might be due to its aberrant subcellular accumulation. Taken together, these results indicate that Cas has an important role in the signaling of axon elongation through interactions with its binding partners via the tyrosine-phosphorylated YDxP motifs.

Phospho-tyrosines within the YDxP motifs are essential for binding Cas to the SH2 domain of the adaptor protein Crk (Zhou *et al.*, 1993; Huang *et al.*, 2002), which subsequently regulates the actin reorganization during fibroblast migration (Klemke *et al.*, 1998). A recent study reported that Crk is recruited to the lipid rafts in growing neurites and mediates lamellipodia formation in PC12 cells (Haglund *et*

al., 2004). Our present data indicate that the interaction between Cas and Crk occurs within the time window when Cas is highly tyrosine-phosphorylated during cerebellar development. In addition, Cas and Crk are subcellularly colocalized with F-actin bundles in the peripheral region of growth cones of cultured granule cells. These results suggest that the impaired axon elongation induced by Cas knockdown with siRNA or overexpression of the ΔYDxP mutant in granule cells might be due to a deficiency in the regulation of the actin-cytoskeletal organization through the YP-Cas-Crk interaction.

Our data demonstrate that JNK1 interacts with the YP-Cas-Crk complex in mouse cerebellum during the early postnatal stage. JNK1 interacts with the SH3 domain of CrkII (Girardin and Yaniv, 2001) and is involved in signaling of neuronal microtubule dynamics through the phosphorylation of microtubule-associated proteins (Chang *et al.*, 2003; Bjorkblom *et al.*, 2005). Another downstream effector of Crk is a small GTPase Rac1 that mediates the actin cytoskeletal dynamics during axonal outgrowth (Luo, 2002). Rac1 is activated by DOCK180, a Crk SH3-binding protein, leading to the lamellipodia formation by fibroblasts (Tanaka *et al.*, 1997; Kiyokawa *et al.*, 1998). It is notable that high Rac activity is present in early postnatal cerebellum (Arakawa *et al.*, 2003). In our primary dissociation cultures, the growth cones of granule cells were very tiny and unstable, and they grew out very rapidly soon after plating on culture dishes. Even if there are subtle changes, it would be very difficult to observe actin dynamics within the growth cone after incubating to obtain effective cellular levels of recombinant Cas proteins, which are exogenously expressed by cDNA transfection. Therefore, we primarily analyzed the length of extending neurites after transfection experiments. Similarly, we did not focus our study on fillopodia and lamellipodia, which are more dynamic structures within the growth cones.

NCAMs actively participate in neurite elongation and dendritic and axonal arbor pathfinding (Walsh and Doherty, 1997; Rougon and Hobert, 2003). The importance of the CAMs, including NCAM, N-cadherin, and L1 for axonal growth was established by a large number of antibody perturbation experiments (Lindner *et al.*, 1983; Hoffman *et al.*, 1986; Walsh and Doherty, 1997; Sakurai *et al.*, 2001; He and Meiri, 2002). A recent study demonstrated that mice deficient for both Nr-CAM and L1 exhibit severe cerebellar folial defects and reduced IGL thickness (Sakurai *et al.*, 2001), indicating that Nr-CAM and L1 have a role in cerebellar granule cell development. Although, to our knowledge, there are no reports of NCAM or N-cadherin knockout mice with defects in cerebellar granule cell development, this might be due to a CAM redundancy. Our data indicate that the developmental expression of N-cadherin and NCAM140/180 mRNA in postnatal mouse cerebella at P7 coincides with that of Cas in the EGL and IGL at the same developmental stage. YP-Cas associates with N-cadherin and NCAMs in the early stage (P3–P12) of cerebellar development, and NCAM and N-cadherin are concentrated in the growth cones of granule cells. Integrin, however, did not coimmunoprecipitate with Cas, which seems to be consistent with a recent study in which NCAM and L1, but not β1 integrin, were detected in the detergent-resistant membranes of cerebellar granule cells (Nakai and Kamiguchi, 2002). NCAM and L1 are implicated in the underlying signaling cascades via the activation of Src and Fyn (Beggs *et al.*, 1994; Ignelzi *et al.*, 1994; Beggs *et al.*, 1997). Whether Cas is tyrosine-phosphorylated after association with CAMs or Cas is tyrosine-phosphorylated before the association with CAMs remain unclear. Cell surface signals via CAMs might activate Src family PTKs, followed by Src PTK binding to and subsequent tyrosine-phosphorylation of Cas protein, leading to the axonal outgrowth of granule cells.

Although Cas mRNAs are localized in both the outer (mitotic) and inner (postmitotic) layer of the EGL, Cas proteins, including phosphorylated form, predominantly distribute in the inner EGL where postmitotic granule cells are settled and begin with their differentiation before cell migration toward the ML. Therefore, we think that Cas is mainly involved in the differentiation of granule cells rather than in the proliferation of their precursors. It is possible, however, that a small amount of Cas protein is involved in granule cell growth.

In conclusion, our data provide functional evidence that the tyrosine-phosphorylated docking protein Cas acts as a signaling interface from the protein tyrosine phosphorylation toward the axonal outgrowth in cerebellar granule cells. The present findings demonstrate that Cas is most abundant in developing mouse cerebellum and is highly tyrosine-phosphorylated in the early postnatal stage, probably by its binding partner Src PTKs. YP-Cas binds Crk, which further recruits downstream proteins such as JNK1. This sequential signaling event likely regulates granule cell axonal outgrowth.

ACKNOWLEDGMENTS

Jinhong Huang was a postdoctoral fellowship recipient of the Japan Society for the Promotion of Science (JSPS). We thank Dr. Noriyuki Morita for the cerebellar dissociation cell cultures and immunohistochemistry, Dr. Fumio Yoshikawa for subcellular fractionation of the growth cone particles, and Dr. Hiroshi Hama for DNA transfection into primary cerebellar neurons. We also thank Dr. Tamae Asawa (National Cancer Research Center) for the Cas siRNA study.

REFERENCES

Arakawa, Y., Bito, H., Furuyashiki, T., Tsuji, T., Takemoto-Kimura, S., Kimura, K., Nozaki, K., Hashimoto, N., and Narumiya, S. (2003). Control of axon elongation via an SDF-1alpha/Rho/mDia pathway in cultured cerebellar granule neurons. J. Cell. Biol. *161*, 381–391.

Azuma, K., Tanaka, M., Uekita, T., Inoue, S., Yokota, J., Ouchi, Y., and Sakai, R. (2005). Tyrosine phosphorylation of paxillin affects the metastatic potential of human osteosarcoma. Oncogene *24*, 4754–4764.

Beggs, H. E., Baragona, S. C., Hemperly, J. J., and Maness, P. F. (1997). NCAM140 interacts with the focal adhesion kinase p125(fak) and the SRC-related tyrosine kinase p59(fyn). J. Biol. Chem. *272*, 8310–8319.

Beggs, H. E., Soriano, P., and Maness, P. F. (1994). NCAM-dependent neurite outgrowth is inhibited in neurons from Fyn-minus mice. J. Cell. Biol. *127*, 825–833.

Bjorkblom, B., Ostman, N., Hongisto, V., Komarovski, V., Filen, J. J., Nyman, T. A., Kallunki, T., Courtney, M. J., and Coffey, E. T. (2005). Constitutively active cytoplasmic c-Jun N-terminal kinase 1 is a dominant regulator of dendritic architecture: role of microtubule-associated protein 2 as an effector. J. Neurosci. *25*, 6350–6361.

Cartwright, C. A., Simantov, R., Cowan, W. M., Hunter, T., and Eckhart, W. (1988). pp60c-src expression in the developing rat brain. Proc. Natl. Acad. Sci. USA *85*, 3348–3352.

Cary, L. A., Han, D. C., Polte, T. R., Hanks, S. K., and Guan, J. L. (1998). Identification of p130Cas as a mediator of focal adhesion kinase-promoted cell migration. J. Cell. Biol. *140*, 211–221.

Chang, L., Jones, Y., Ellisman, M. H., Goldstein, L. S., and Karin, M. (2003). JNK1 is required for maintenance of neuronal microtubules and controls phosphorylation of microtubule-associated proteins. Dev. Cell. *4*, 521–533.

Chen, S., Ren, Y. Q., and Hillman, D. E. (1996). Transient expression of lyn gene in Purkinje cells during cerebellar development. Brain Res. Dev. Brain Res. *92*, 140–146.

Dent, E. W., and Gertler, F. B. (2003). Cytoskeletal dynamics and transport in growth cone motility and axon guidance. Neuron *40*, 209–227.

Dickson, B. J. (2001). Rho GTPases in growth cone guidance. Curr. Opin. Neurobiol. *11*, 103–110.

Fults, D. W., Towle, A. C., Lauder, J. M., and Maness, P. F. (1985). pp60c-src in the developing cerebellum. Mol. Cell. Biol. *5*, 27–32.

Girardin, S. E., and Yaniv, M. (2001). A direct interaction between JNK1 and CrkII is critical for Rac1-induced JNK activation. EMBO J. *20*, 3437–3446.

Haglund, K., Ivankovic-Dikic, I., Shimokawa, N., Kruh, G. D., and Dikic, I. (2004). Recruitment of Pyk2 and Cbl to lipid rafts mediates signals important for actin reorganization in growing neurites. J. Cell. Sci. *117*, 2557–2568.

Hama, H., Hara, C., Yamaguchi, K., and Miyawaki, A. (2004). Protein kinase C signaling mediates global enhancement of excitatory synaptogenesis in neurons triggered by local contact with astrocytes. Neuron *41*, 405–415.

Hatten, M. E., and Heintz, N. (1995). Mechanisms of neural patterning and specification in the developing cerebellum. Annu. Rev. Neurosci. *18*, 385–408.

He, Q., and Meiri, K. F. (2002). Isolation and characterization of detergent-resistant microdomains responsive to NCAM-mediated signaling from growth cones. Mol. Cell. Neurosci. *19*, 18–31.

Helmke, S., Lohse, K., Mikule, K., Wood, M. R., and Pfenninger, K. H. (1998). SRC binding to the cytoskeleton, triggered by growth cone attachment to laminin, is protein tyrosine phosphatase-dependent. J. Cell. Sci. *111*(Pt 16), 2465–2475.

Hoffman, S., Friedlander, D. R., Chuong, C. M., Grumet, M., and Edelman, G. M. (1986). Differential contributions of Ng-CAM and N-CAM to cell adhesion in different neural regions. J. Cell. Biol. *103*, 145–158.

Honda, H. *et al.* (1998). Cardiovascular anomaly, impaired actin bundling and resistance to Src-induced transformation in mice lacking p130Cas. Nat. Genet. *19*, 361–365.

Huang, J., Hamasaki, H., Nakamoto, T., Honda, H., Hirai, H., Saito, M., Takato, T., and Sakai, R. (2002). Differential regulation of cell migration, actin stress fiber organization, and cell transformation by functional domains of Crk-associated substrate. J. Biol. Chem. *277*, 27265–27272.

Ignelzi, M. A., Jr., Miller, D. R., Soriano, P., and Maness, P. F. (1994). Impaired neurite outgrowth of src-minus cerebellar neurons on the cell adhesion molecule L1. Neuron *12*, 873–884.

Kiyokawa, E., Hashimoto, Y., Kobayashi, S., Sugimura, H., Kurata, T., and Matsuda, M. (1998). Activation of Rac1 by a Crk SH3-binding protein, DOCK180. Genes Dev. *12*, 3331–3336.

Klemke, R. L., Leng, J., Molander, R., Brooks, P. C., Vuori, K., and Cheresh, D. A. (1998). CAS/Crk coupling serves as a "molecular switch" for induction of cell migration. J. Cell Biol. *140*, 961–972.

Korey, C. A., and Van Vactor, D. (2000). From the growth cone surface to the cytoskeleton: one journey, many paths. J. Neurobiol. *44*, 184–193.

Lindner, J., Rathjen, F. G., and Schachner, M. (1983). L1 mono- and polyclonal antibodies modify cell migration in early postnatal mouse cerebellum. Nature *305*, 427–430.

Liu, J. J., Ding, J., Kowal, A. S., Nardine, T., Allen, E., Delcroix, J. D., Wu, C., Mobley, W., Fuchs, E., and Yang, Y. (2003). BPAG1n4 is essential for retrograde axonal transport in sensory neurons. J. Cell. Biol. *163*, 223–229.

Luo, L. (2002). Actin cytoskeleton regulation in neuronal morphogenesis and structural plasticity. Annu. Rev. Cell Dev. Biol. *18*, 601–635.

Maness, P. F., Aubry, M., Shores, C. G., Frame, L., and Pfenninger, K. H. (1988). c-src gene product in developing rat brain is enriched in nerve growth cone membranes. Proc. Natl. Acad. Sci. USA *85*, 5001–5005.

Miyake, I., Hakomori, Y., Misu, Y., Nakadate, H., Matsuura, N., Sakamoto, M., and Sakai, R. (2005). Domain-specific function of ShcC docking protein in neuroblastoma cells. Oncogene *24*, 3206–3215.

Nakai, Y., and Kamiguchi, H. (2002). Migration of nerve growth cones requires detergent-resistant membranes in a spatially defined and substrate-dependent manner. J. Cell Biol. *159*, 1097–1108.

Nakamoto, T., Sakai, R., Ozawa, K., Yazaki, Y., and Hirai, H. (1996). Direct binding of C-terminal region of p130Cas to SH2 and SH3 domains of Src kinase. J. Biol. Chem. *271*, 8959–8965.

O'Neill, G. M., Fashena, S. J., and Golemis, E. A. (2000). Integrin signalling: a new Cas. (t) of characters enters the stage. Trends Cell Biol. *10*, 111–119.

Omri, B., Crisanti, P., Marty, M. C., Alliot, F., Fagard, R., Molina, T., and Pessac, B. (1996). The Lck tyrosine kinase is expressed in brain neurons. J. Neurochem. *67*, 1360–1364.

Ono, K., Shokunbi, T., Nagata, I., Tokunaga, A., Yasui, Y., and Nakatsuji, N. (1997). Filopodia and growth cones in the vertically migrating granule cells of the postnatal mouse cerebellum. Exp. Brain Res. *117*, 17–29.

Pellicena, P., and Miller, W. T. (2001). Processive phosphorylation of p130Cas by Src depends on SH3-polyproline interactions. J. Biol. Chem. *276*, 28190–28196.

Pfenninger, K. H., Ellis, L., Johnson, M. P., Friedman, L. B., and Somlo, S. (1983). Nerve growth cones isolated from fetal rat brain: subcellular fractionation and characterization. Cell *35*, 573–584.

Pollard, T. D., and Borisy, G. G. (2003). Cellular motility driven by assembly and disassembly of actin filaments. Cell *112*, 453–465.

Powell, S. K., Rivas, R. J., Rodriguez-Boulan, E., and Hatten, M. E. (1997). Development of polarity in cerebellar granule neurons. J. Neurobiol. *32*, 223–236.

Ribon, V., and Saltiel, A. R. (1996). Nerve growth factor stimulates the tyrosine phosphorylation of endogenous Crk-II and augments its association with p130Cas in PC-12 cells. J. Biol. Chem. *271*, 7375–7380.

Rico, B., Beggs, H. E., Schahin-Reed, D., Kimes, N., Schmidt, A., and Reichardt, L. F. (2004). Control of axonal branching and synapse formation by focal adhesion kinase. Nat. Neurosci. *7*, 1059–1069.

Rougon, G., and Hobert, O. (2003). New insights into the diversity and function of neuronal immunoglobulin (Ig) superfamily molecules. Annu. Rev. Neurosci. *26*, 207–238.

Ruest, P. J., Shin, N. Y., Polte, T. R., Zhang, X., and Hanks, S. K. (2001). Mechanisms of CAS substrate domain tyrosine phosphorylation by FAK and Src. Mol. Cell. Biol. *21*, 7641–7652.

Sakai, R., Iwamatsu, A., Hirano, N., Ogawa, S., Tanaka, T., Mano, H., Yazaki, Y., and Hirai, H. (1994). A novel signaling molecule, p130, forms stable complexes in vivo with v-Crk and v-Src in a tyrosine phosphorylation-dependent manner. EMBO J. *13*, 3748–3756.

Sakurai, T., Lustig, M., Babiarz, J., Furley, A. J., Tait, S., Brophy, P. J., Brown, S. A., Brown, L. Y., Mason, C. A., and Grumet, M. (2001). Overlapping functions of the cell adhesion molecules Nr-CAM and L1 in cerebellar granule cell development. J. Cell Biol. *154*, 1259–1273.

Shiraishi, Y., Mizutani, A., Bito, H., Fujisawa, K., Narumiya, S., Mikoshiba, K., and Furuichi, T. (1999). Cupidin, an isoform of Homer/Vesl, interacts with the actin cytoskeleton and activated rho family small GTPases and is expressed in developing mouse cerebellar granule cells. J. Neurosci. *19*, 8389–8400.

Sudol, M., Alvarez-Buylla, A., and Hanafusa, H. (1988). Differential developmental expression of cellular yes and cellular src proteins in cerebellum. Oncogene Res. *2*, 345–355.

Sudol, M., Kuo, C. F., Shigemitsu, L., and Alvarez-Buylla, A. (1989). Expression of the yes proto-oncogene in cerebellar Purkinje cells. Mol. Cell. Biol. *9*, 4545–4549.

Tanaka, E., and Sabry, J. (1995). Making the connection: cytoskeletal rearrangements during growth cone guidance. Cell *83*, 171–176.

Tanaka, S., Ouchi, T., and Hanafusa, H. (1997). Downstream of Crk adaptor signaling pathway: activation of Jun kinase by v-Crk through the guanine nucleotide exchange protein C3G. Proc. Natl. Acad. Sci. USA *94*, 2356–2361.

Walsh, F. S., and Doherty, P. (1997). Neural cell adhesion molecules of the Ig superfamily: role in axon growth and guidance. Annu. Rev. Cell Dev. Biol. *13*, 425–456.

Wu, D. Y., and Goldberg, D. J. (1993). Regulated tyrosine phosphorylation at the tips of growth cone filopodia. J. Cell Biol. *123*, 653–664.

Zhao, Y. H., Baker, H., Walaas, S. I., and Sudol, M. (1991). Localization of p62c-yes protein in mammalian neural tissues. Oncogene *6*, 1725–1733.

Zhou, S., Shoelson, S. E., Chaudhuri, M., Gish, G., Pawson, T., Haser, W. G., King, F., Roberts, T., Ratnofsky, S., and Lechleider, R. J. (1993). SH2 domains recognize specific phosphopeptide sequences. Cell *72*, 767–778.

Cell

Force Sensing by Mechanical Extension of the Src Family Kinase Substrate p130Cas

Yasuhiro Sawada,[1,*] Masako Tamada,[1] Benjamin J. Dubin-Thaler,[1] Oksana Cherniavskaya,[1] Ryuichi Sakai,[2] Sakae Tanaka,[3] and Michael P. Sheetz[1]
[1]Department of Biological Sciences, Columbia University, Sherman Fairchild Center Room 715, MC-2416, 1212 Amsterdam Avenue, New York, NY 10027, USA
[2]Growth Factor Division, National Cancer Center Research Institute, 5-1-1 Tsukiji, Chuo-ku, Tokyo 104-0045, Japan
[3]Department of Orthopaedic Surgery, Graduate School of Medicine, The University of Tokyo, 7-3-1 Hongo, Bunkyo-ku, Tokyo 113-0033, Japan
*Contact: ys454-ind@umin.ac.jp
DOI 10.1016/j.cell.2006.09.044

SUMMARY

How physical force is sensed by cells and transduced into cellular signaling pathways is poorly understood. Previously, we showed that tyrosine phosphorylation of p130Cas (Cas) in a cytoskeletal complex is involved in force-dependent activation of the small GTPase Rap1. Here, we mechanically extended bacterially expressed Cas substrate domain protein (CasSD) in vitro and found a remarkable enhancement of phosphorylation by Src family kinases with no apparent change in kinase activity. Using an antibody that recognized extended CasSD in vitro, we observed Cas extension in intact cells in the peripheral regions of spreading cells, where higher traction forces are expected and where phosphorylated Cas was detected, suggesting that the in vitro extension and phosphorylation of CasSD are relevant to physiological force transduction. Thus, we propose that Cas acts as a primary force sensor, transducing force into mechanical extension and thereby priming phosphorylation and activation of downstream signaling.

INTRODUCTION

Cellular responses to mechanical force underlie many critical functions, from normal morphogenesis to carcinogenesis, cardiac hypertrophy, wound healing, and bone homeostasis. Recent studies indicate that various signaling pathways are involved in force transduction, including MAP kinases, small GTPases, and tyrosine kinases/phosphatases (Geiger and Bershadsky, 2002; Giannone and Sheetz, 2006; Katsumi et al., 2002; Sawada et al., 2001). A variety of primary force-sensing mechanisms could be postulated, including mechanical extension of cytoplasmic proteins, activation of ion channels, and formation of force-stabilized receptor-ligand bonds (catch bonds) (Vogel and Sheetz, 2006), which would then activate downstream signaling pathways. At a biochemical level, tyrosine phosphorylation levels appear to be linked to mechanically induced changes controlling many other cellular functions (Giannone and Sheetz, 2006). One protein involved in mechanically induced phosphorylation-dependent signaling is the Src family kinase substrate Cas (Crk-*a*ssociated *s*ubstrate), which is involved in various cellular events such as migration, survival, transformation, and invasion (Defilippi et al., 2006). Stretch-dependent tyrosine phosphorylation of Cas by Src family kinases (SFKs) occurs in detergent-insoluble cytoskeletal complexes and is involved in force-dependent activation of the small GTPase Rap1 (Tamada et al., 2004). Rap1 is activated by distinct types of guanine nucleotide exchange factors coupled with various receptors or second messengers and plays an important role in a number of signaling pathways, including integrin signaling (Hattori and Minato, 2003).

The Cas substrate domain, which is located in the center of Cas, is flanked by the amino-terminal SH3 and the carboxy-terminal Src-binding domains. These amino- and carboxy-terminal domains are involved in Cas localization at focal adhesions, while the substrate domain itself is not (Nakamoto et al., 1997), suggesting that these flanking domains anchor Cas molecules to the cytoskeletal complex and that the substrate domain could be extended upon cytoskeleton stretching. Furthermore, the Cas substrate domain has 15 repeats of a tyrosine-containing motif (YxxP) (Mayer et al., 1995), and multiple sequence repeats are found in molecules with mechanical functions such as titin (Rief et al., 1997).

Cell stretching could increase tyrosine phosphorylation by (1) directly activating the kinase, (2) inactivating the phosphatase, (3) mechanically bringing the kinase to the substrate, or (4) enhancing the susceptibility of the substrate to phosphorylation. To test between these possibilities, we have analyzed the mechanisms of stretch-dependent

enhancement of Cas phosphorylation. In intact cells, Cas phosphorylation by c-Src is significantly increased by cell stretching with no detectable change in c-Src kinase activity. Cas phosphorylation mediates physiological force transduction through stretch-dependent activation of Rap1 in intact cells. With *in* vitro *p*rotein *e*xtension (IPE) experiments, we find that phosphorylation of CasSD by specific kinases is increased upon extension. Further, an antibody that recognizes extended CasSD in vitro preferentially recognizes Cas molecules at the periphery of late spreading cells where higher traction forces are predicted and Cas is phosphorylated, indicating that the in vitro extension and phosphorylation of CasSD is relevant to force transduction through Cas phosphorylation in intact cells. Thus, we suggest that Cas serves as a direct mechanosensor where force induces a mechanical extension of the substrate domain that primes it for phosphorylation. We propose that such "substrate priming" is a general mechanism for force transduction.

RESULTS

Cell Stretching Enhances SFK-Dependent Phosphorylation of Cas without a Detectable Increase in Src Kinase Activity

We first examined whether the phosphorylation of Cas increased upon intact cell stretching, using the cell stretching system that we developed (Sawada et al., 2001). Cells were cultured on a stretchable substrate (collagen-coated silicone), and the substrate was stretched uniformly and biaxially (10% in each dimension) and held stretched. To analyze the primary responses to cell stretching, samples were prepared from the cells lysed shortly (1 min) after stretching. Immunoblotting using an anti-phospho-Cas antibody (pCas-165) that specifically recognizes multiple phosphorylated YxxP motifs in the substrate domain (Fonseca et al., 2004) revealed a stretch-dependent increase in tyrosine phosphorylation of Cas in HEK293 cells (Figure 1A). When the selective SFK inhibitor CGP77675 (Missbach et al., 1999) (Novartis Pharma AG, Switzerland) was added prior to stretching, stretch-dependent tyrosine phosphorylation of Cas was inhibited (Figure 1A). Furthermore, stretch-dependent phosphorylation of Cas was greatly attenuated in SYF cells that lacked the major SFKs, c-Src, c-Yes, and Fyn (Klinghoffer et al., 1999), and was restored in SYF cells stably expressing c-Src (Figure 1B), c-Yes, or Fyn (data not shown). Thus, stretching intact cells increased tyrosine phosphorylation of Cas by SFKs.

To determine if stretch-dependent increases in Cas phosphorylation correlated with SFK activation, the levels of c-Src phosphorylation at either activating or inhibiting tyrosine residue (Y416 and Y527, respectively) were examined in SYF cells stably expressing c-Src, either stretched or left unstretched. We observed no changes in phosphorylation levels of those tyrosines (pY416 and pY527) (Figure 1B, lanes 3 and 4). Since the levels of pY416 and pY527 indicate Src kinase inhibition and activation, respectively (Thomas and Brugge, 1997), cell stretching did not appear to affect c-Src activity, while Cas phosphorylation significantly increased. This was further confirmed by an in vitro kinase assay of immunoprecipitated c-Src (Figure 1C). Thus, stretching intact cells increased tyrosine phosphorylation of Cas by c-Src without detectable enhancement of c-Src kinase activity.

Tyrosine Phosphorylation of Cas Is Involved in Stretch-Dependent Rap1 Activation

To explore the role of Cas in physiological force transduction pathways, we analyzed the involvement of Cas in the stretch-dependent activation of Rap1 in cells (Sawada et al., 2001). When the level of Cas protein and phosphorylated Cas was selectively decreased by small interfering RNA (siRNA) in HEK293 cells (Figure 2A, upper panel), Rap1 activity in cells, either stretched or unstretched, was significantly attenuated (Figure 2A, lower panel). Thus, Cas plays a significant role in the stretch-dependent activation of Rap1 in intact cells. However, there is likely more than one pathway for Rap1 activation, considering the fold decrease of Rap1 activity (~50%) in Cas knockdown cells (Figure 2A) as well as the stretch-dependent Rap1 activation observed in Cas-deficient fibroblasts (data not shown).

To further examine the role of phosphorylation of Cas in stretch-dependent Rap1 activation, we overexpressed Cas together with Rap1 in HEK293 cells. Upon coexpression of monomeric red fluorescent protein (RFP)-tagged wild-type Cas (RFP-Cas) with green fluorescent protein (GFP)-tagged Rap1 (GFP-Rap1), stretch-dependent activity of GFP-Rap1 was enhanced over the cells coexpressing RFP alone or RFP-Cas15YF that had all 15 YxxP motifs in the substrate domain mutated to FxxP (Figure 2B). The fold increase of Rap1 activity by cell stretching appeared to be smaller in the case of RFP-Cas-expressing cells, probably due to the less efficient incorporation of "overexpressed" Cas into physiological signaling complexes. However, we conclude that tyrosine phosphorylation of Cas is responsible for a significant fraction of the stretch-dependent Rap1 activation.

In Vitro Extension of CasSD

Because kinase activation did not appear to be the primary mechanism regulating Cas phosphorylation in response to cell stretching (Figures 1B and 1C), we tested whether the mechanical extension of the Cas substrate domain modulated its susceptibility to phosphorylation by SFKs. To eliminate the involvement of any extraneous molecules, we performed biochemical analysis, using an IPE system. In that system, bacterially expressed Cas substrate domain protein, CasSD (Cas115–420), was biotinylated on both amino and carboxy termini (designated NC-biotinylated CasSD, Figure 3A, top) and was bound to avidin covalently immobilized on a latex substrate (Figure 3A). After stretching of the latex membrane (Figure 3A), biochemical analyses were performed.

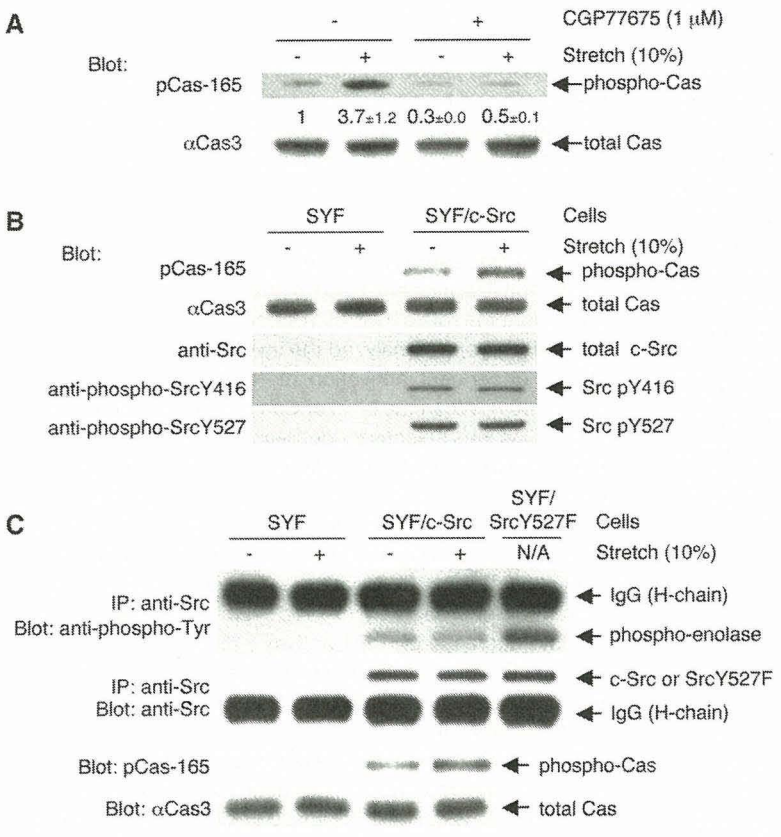

Figure 1. SFK- and Stretch-Dependent Tyrosine Phosphorylation of Cas In Vivo

(A) Stretch-dependent tyrosine phosphorylation of Cas in intact cells. HEK293 (2×10^5) cells on the collagen (type I)-coated stretchable silicone dish were treated with either CGP77675 (1 μM) or its vehicle (0.01% DMSO) and were either stretched (biaxially, 10% in each dimension) or left unstretched. One minute after stretching or without stretching, the cells were solubilized with 1× SDS sample buffer containing 20 mM DTT and analyzed for Cas phosphorylation by anti-phospho-Cas (pCas-165) and anti-Cas (αCas3) immunoblotting. Quantification of phosphorylation (phospho-Cas/total Cas) was scaled with unstretched control set at 1 and noted below the pCas-165 blot with SD (n = 4).

(B) Cell stretching increases Src-dependent phosphorylation of Cas without apparent change in phosphorylation levels of activating and inhibiting tyrosines of c-Src. SYF cells (triple knockout cells of c-src, c-yes, and fyn) or SYF cells stably expressing c-Src (4×10^5) were either stretched or left unstretched. One minute after stretching or without stretching, cells were solubilized with SDS sample buffer, and equivalent portions of each sample were subjected to SDS-PAGE followed by pCas-165, αCas3, anti-Src, anti-phospho-Src Y416, and anti-phospho-Src Y527 immunoblotting.

(C) Cell stretching increases Src-dependent phosphorylation of Cas without apparent change in Src kinase activity. SYF cells or SYF cells stably expressing c-Src (4×10^5) were either stretched or left unstretched. One minute after stretching or without stretching, cells were lysed and subjected to immunoprecipitation followed by an in vitro kinase assay using acid-treated enolase as a substrate. Src kinase activity was analyzed by measuring the phosphorylation of enolase with anti-phospho-tyrosine immunoblotting (top panel). Immunoprecipitated Src, i.e., Src protein in the kinase reaction, was quantified by anti-Src immunoblotting (second panel). Equivalent small portions of each lysate were mixed with SDS sample buffer and subjected directly to SDS-PAGE followed by pCas-165 and αCas3 immunoblotting to analyze for Cas phosphorylation (third and fourth panels). Kinase reactions for the lane 3 and 4 samples appeared not to be saturated because the sample prepared from SYF/SrcY527F cells (SYF cells expressing SrcY527F, the highly active mutant form of c-Src) cultured on a plastic plate following the same protocol gave more phosphorylation of enolase (lane 5). The intense bands above enolase (top panel) and below Src (second panel) represent IgG (heavy chain) from the anti-Src antibody.

To determine if stretching of the latex membrane actually extended NC-biotinylated CasSD, we developed the yellow fluorescent protein (YFP) amino-terminal swapping assay based on the interaction between the amino- and carboxy-terminal regions of YFP. In this assay, CasSD extension was detected by the separation of YFP components attached to the ends of CasSD, causing the binding of an exogenous YFP component. When the two halves of a split YFP, YFP-N and YFP-C, were fused to the amino- and carboxy-terminal ends of NC-biotinylated CasSD, respectively (NY/CY-NC-biotinylated CasSD, Figure 3B), we observed yellow fluorescence in both NY/CY-NC-biotinylated CasSD-expressing bacteria and the purified protein, as expected (Hu et al., 2002). When we added purified His_6-YFP-N to bind to YFP-C in NY/CY-NC biotinylated CasSD (Figure 3B, top), His_6-YFP-N binding was not observed without latex membrane stretching (Figure 3C, lane 1). However, we observed His_6-YFP-N binding upon stretching (Figure 3C, lane 2). Furthermore, His_6-YFP-N did not bind to NY/CY-C-biotinylated CasSD (the unextendable mono-biotinylated control, Figure 3B, bottom) or NC-biotinylated CasSD (extendable, but with no YFP component, Figure 3A, top) even following stretching (Figure 3C, lanes 3–6). Using His_6-YFP-N together with YFP-C fused to glutathione *S*-transferase (GST) in a GST pull-down experiment, we found that YFP-N bound to YFP-C under the same buffer conditions used in the YFP amino-terminal swapping assay (data not shown). Thus, stretching of the latex membrane separated the YFP halves in NY/CY-NC-biotinylated CasSD and allowed His_6-YFP-N to bind, indicating the extension of CasSD (Figure 3B, top).

Extension-Dependent Phosphorylation of CasSD by Recombinant Tyrosine Kinases In Vitro

Since CasSD could be extended by the IPE system, we examined the effect of extension on tyrosine phosphorylation of CasSD by recombinant active c-Src. While the level of phosphorylation was low without stretching (Figure 4A, lane 1), CasSD phosphorylation increased in proportion

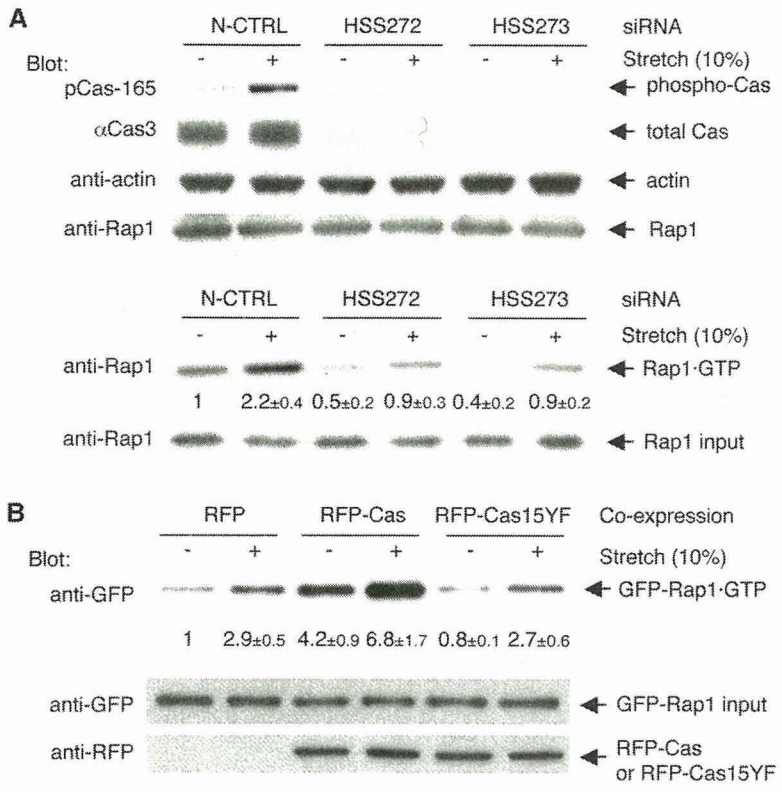

Figure 2. Significant Role of Cas Phosphorylation in Physiological Force Transduction

(A) Cas is involved in stretch-dependent Rap1 activation in intact cells. RNAi experiments were performed as described in the Experimental Procedures. siRNAs used were Stealth RNAi Negative Control Med GC (N-CTRL: lanes 1 and 2), BCAR1-HSS114272 (HSS272: lanes 3 and 4), and BCAR1-HSS114273 (HSS273: lanes 5 and 6) (Invitrogen). Twenty-four hours after transfection, HEK293 cells were either stretched or left unstretched. To determine the level of Cas expression and phosphorylation, cells were solubilized with SDS sample buffer 1 min after stretching or without stretching, and equivalent portions of each sample were subjected to SDS-PAGE followed by anti-phospho-Cas (pCas-165), anti-Cas (αCas3), anti-Rap1, and anti-actin immunoblotting (upper panel). To measure stretch-dependent Rap1 activity, cells were solubilized with lysis buffer for GST pull-down assay (see Experimental Procedures) 5 min after stretching or without stretching. Rap1 was quantified by anti-Rap1 immunoblotting. Rap1 activity (Rap1•GTP/Rap1 input) was scaled with the unstretched control set at 1 and noted below the Rap1•GTP blot with SD (n = 4) (lower panel). The data shown in Figure 2A (upper and lower panels) were obtained with siRNA transfection performed at the same time.

(B) Significant role of tyrosine phosphorylation of Cas in stretch-dependent Rap1 activation. RFP, RFP-Cas, or RFP-Cas15YF was cotransfected with GFP-Rap1 into HEK293 cells (1×10^5/dish). Twenty-four hours after transfection, cells were either stretched or left unstretched. Five minutes after stretching or without stretching, cells were solubilized and subjected to the GST pull-down assay. GFP-Rap1 was quantified by anti-GFP immunoblotting. GFP-Rap1 activity (GFP-Rap1•GTP/GFP-Rap1 input) was scaled with the unstretched RFP-transfected cells set at 1 and noted below the GFP-Rap1•GTP blot with SD (n = 4).

to the magnitude of latex membrane stretching (25%, 50%, 75%, 100%, and 150%) (Figure 4A, lanes 2–6). An unextendable mono-biotinylated CasSD (C-biotinylated CasSD, see Figure 3A, top) was poorly tyrosine phosphorylated either with or without stretching (Figure 4A, lanes 7 and 8). To test if c-Src kinase activity was modulated in the IPE experiments, we added acid-treated enolase to the kinase mixture at the time of kinase reaction and measured its phosphorylation. In the same reaction that gave an extension-dependent increase in CasSD phosphorylation, neither the level of enolase phosphorylation nor the phosphorylation levels of Y416 and Y527 of c-Src kinase were affected by stretching (data not shown). These results indicated that extension-dependent tyrosine phosphorylation of CasSD resulted from CasSD extension and not from an increase in the kinase activity of recombinant c-Src.

We also asked whether or not other kinases phosphorylated CasSD in an extension-dependent manner in IPE experiments. Neither the non-SFK tyrosine kinase Csk (C-terminal Src kinase) nor ZAP-70 phosphorylated NC-biotinylated CasSD, even after stretching (Figure 4B). However, in the same kinase reaction protocol, both Csk and ZAP-70 were able to phosphorylate their known substrates, acid-treated enolase (Bougeret et al., 1993) and the cytoplasmic fragment of human erythrocyte band 3 (cdb3) (Isakov et al., 1996), respectively (data not shown). On the other hand, a known Cas kinase, Abl (Mayer et al., 1995) and another SFK, FynT, phosphorylated CasSD in an extension-dependent manner (Figure 4B). Thus, extension-dependent phosphorylation of CasSD in vitro is caused in a kinase-specific manner, and not by a nonspecific effect of the IPE system.

Although neither the force needed for CasSD extension nor its effect on individual YxxP motifs in CasSD is known, the IPE experiments revealed that different extents of extension induced the phosphorylation of different regions. When we used two different anti-phospho-Cas antibodies (pCas-165 and pCas-410) that had different, though not strictly specific, binding preferences for YxxPs in the Cas substrate domain (Shin et al., 2004) to measure the in vitro CasSD phosphorylation, pCas-410 immunoblotting gave significantly greater fold increase than pCas-165 blots by 40% latex membrane stretching (Figure 4C, left panel). However, pCas-165 and pCas-410 blots showed a similar fold increase by 100% stretching (Figure 4C, right panel). These results suggest that the pCas-410 sites are more efficiently exposed and phosphorylated than pCas-165 sites by smaller extent of CasSD extension.

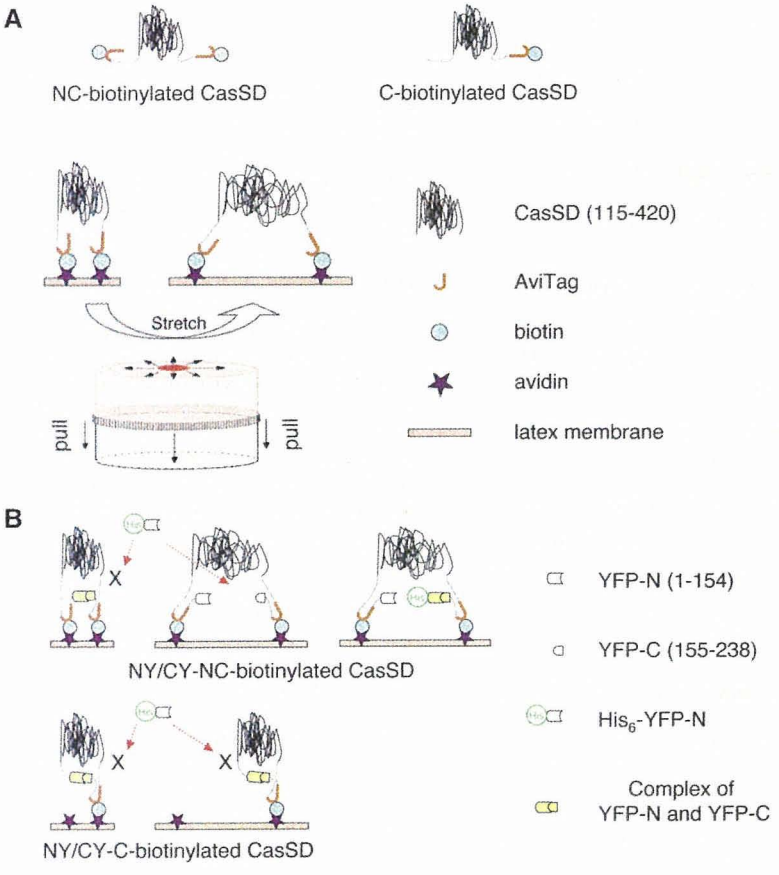

Figure 3. IPE System

(A) Scheme of NC-biotinylated CasSD, C-biotinylated CasSD, and the process of mechanical extension of CasSD in the IPE system.

(B) Schematic description of YFP amino-terminal swapping.

(C) His_6-YFP-N binds to extended NY/CY-NC-biotinylated CasSD, but not to NY/CY-C-biotinylated CasSD or NC-biotinylated CasSD. Biotinylated CasSD proteins, either extended or unextended on latex membrane, were incubated with His_6-YFP-N in the buffer containing 1% Triton X-100 and 1% BSA. After washing, bound complex was solubilized and subjected to SDS-PAGE followed by anti-polyHistidine immunoblotting or avidin affinity blotting.

αCas1, an Antibody that Recognizes Extended CasSD

In order to test if Cas was extended in regions of cell traction forces, we utilized an antibody, αCas1, which was raised against a peptide sequence in the Cas substrate domain (Sakai et al., 1994) (Figure S1A). We found that αCas1 recognized the extended NC-biotinylated CasSD and not the unextended control, C-biotinylated CasSD in the IPE system (Figure 5A). Further, αCas1 bound to SDS-denatured CasSD regardless of its phosphorylation state (Figure S1B), as well as full-length Cas in the SDS-denatured cell lysates (Figure S1C). Thus, αCas1 binding appeared to require the exposure of its epitope in the Cas substrate domain by either extension or denaturation.

Extension of Cas in Triton Cytoskeletons

Using αCas1, we examined whether Cas was extended by stretching Triton cytoskeletons where tyrosine phosphorylation of Cas was observed (Tamada et al., 2004). When we stretched Triton cytoskeletons from Cas-deficient fibroblasts expressing RFP-Cas, we observed a significant increase in αCas1 binding (Figure 5B, lower panel, lanes 1 and 2). Triton cytoskeletons from Cas-deficient fibroblasts expressing RFP alone did not bind αCas1 (Figure 5B, lower panel, lanes 3 and 4). Further, another anti-Cas antibody, αCas3, the epitope of which did not involve the substrate domain (Figure S1A) (Sakai et al., 1994), did not change its binding to Cas in Triton cytoskeletons upon stretching (Figure 5B, lower panel, lanes 5 and 6). These results indicate that the extension of the Cas substrate domain is enhanced by cytoskeleton stretching.

Cas Is Extended at the Sites of High Traction Forces Where Cas Is Phosphorylated In Vivo

Cas extension was difficult to observe in intact cells, since the cell stretching system could not fit onto a total internal

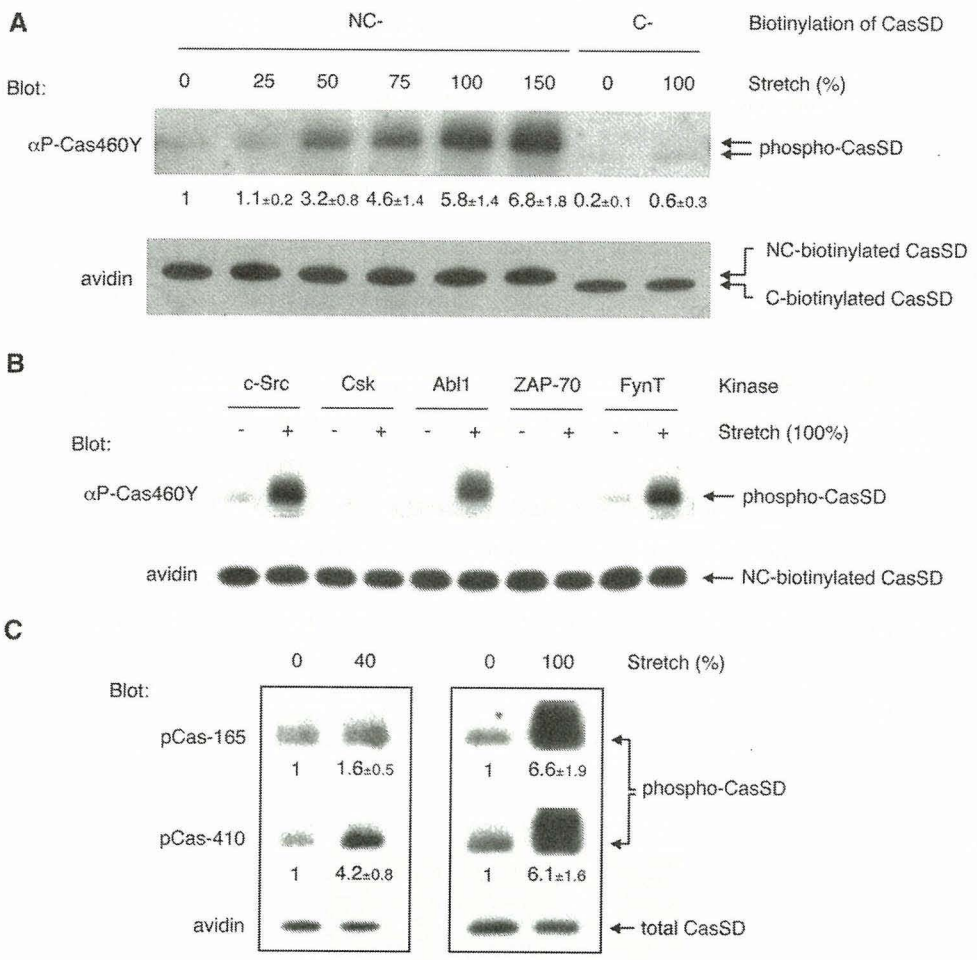

Figure 4. Extension-Dependent Phosphorylation of CasSD by Tyrosine Kinases In Vitro

(A) CasSD is tyrosine phosphorylated by recombinant c-Src in an extension-dependent manner. NC-biotinylated or C-biotinylated CasSD was either extended or left unextended on latex membrane, incubated with recombinant c-Src for 2 min, washed, solubilized, and analyzed for tyrosine phosphorylation by anti-phospho-Cas (αP-Cas460Y) immunoblotting and avidin affinity blotting. The magnitude of the latex membrane stretching is described as the percent change of length in each dimension. Quantification of phosphorylation of CasSD was scaled with unextended NC-biotinylated CasSD set at 1 and noted below the anti-phospho-Cas blot with SD (n = 4).

(B) Kinase specificity of extension-dependent tyrosine phosphorylation of CasSD. NC-biotinylated CasSD was either extended (100%) or left unextended and then incubated with recombinant c-Src, Csk, Abl1, ZAP-70, or FynT for 2 min at room temperature. Tyrosine phosphorylation of CasSD was analyzed as in (A).

(C) Extension-dependent phosphorylation of CasSD by c-Src measured by two different anti-phospho-Cas antibodies. Samples were prepared as in (A) except for the extent of the latex membrane stretching (40% in the left panel and 100% in the right panel). Equivalent portions of each sample were subjected to SDS-PAGE followed by pCas-165 and pCas-410 immunoblotting and avidin affinity blotting. Quantification of phosphorylation of CasSD was scaled with unextended NC-biotinylated CasSD set at 1 and noted below the anti-phospho-Cas blots with SD (n = 4).

reflection fluorescence (TIRF) or confocal microscope. Further, the stretchable substrate (silicone) had high background fluorescence. Therefore, we looked at αCas1 immunostaining of intact cells during the late phase of spreading on collagen-coated glass coverslips (20 min after plating), when the fast movement of actin cytoskeletons at the periphery is observed (Dubin-Thaler et al., 2004) and the forces required for continuous spreading are generated (Giannone et al., 2004). In RFP-Cas-expressing Cas-deficient fibroblasts, we found that αCas1 staining primarily colocalized with RFP-Cas in the peripheral regions (Figure 5C, top). An anti-phospho-Cas antibody (pCas-165) also exhibited a peripheral staining in the late spreading cells (Figure 5C, bottom), confirming that Cas extension correlated with phosphorylation. These staining patterns did not appear to be artifacts of antibody staining, since αCas3 staining always colocalized with RFP-Cas (Figure 5C, middle). Considering the specificity of αCas1 and αCas3 in immunoblotting (Figure S1C), both αCas1 and αCas3 staining most likely represent the distribution of their Cas epitopes, and not the crossreaction with other cellular protein(s). Indeed, we observed

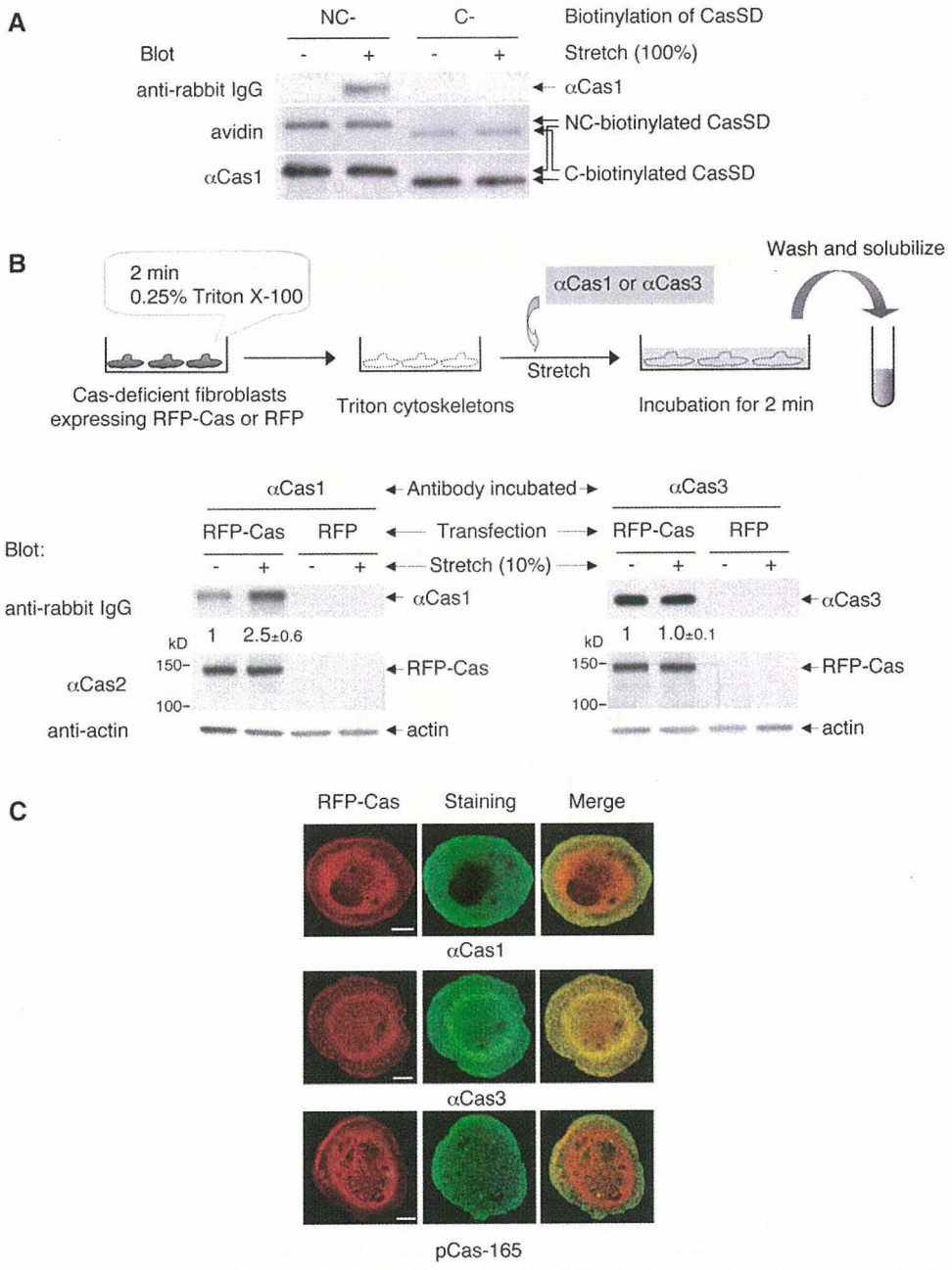

Figure 5. Extension of Cas In Situ and In Vivo

(A) αCas1 recognizes extended CasSD in vitro. NC-biotinylated or C-biotinylated CasSD was either extended (100%) or left unextended in the IPE system. After blocking, CasSD proteins were incubated with αCas1, washed, and solubilized with SDS sample buffer containing 0.12 M DTT. Equivalent portions of each sample were analyzed for quantification of bound αCas1 by anti-rabbit IgG immunoblotting. The amount of NC-biotinylated and C-biotinylated CasSD in each sample was quantified by avidin affinity blotting and αCas1 immunoblotting. Note that the difference in the relative signal intensity between avidin and αCas1 blots is consistent with the molar ratio of biotinylation (NC-biotinylated CasSD:C-biotinylated CasSD = 2:1).

(B) Stretch dependence of αCas1 and αCas3 binding to Cas in Triton cytoskeletons. Triton cytoskeletons were prepared from Cas-deficient fibroblasts transfected with RFP-Cas or RFP alone, either stretched or left unstretched, and incubated with either αCas1 or αCas3 as shown in the diagram. Quantification of bound antibody by anti-rabbit IgG immunoblotting was scaled with unstretched control set at 1 and noted with SD (n = 4).

(C) αCas1 preferentially binds to Cas, where higher traction forces are expected in vivo. Cas-deficient fibroblasts expressing RFP-Cas were plated, fixed after 20 min, and then stained with αCas1, αCas3, or pCas-165. Confocal images are shown for RFP-Cas (left, red channel) and immunostaining (center, green channel) and are merged on the right. Scale bars, 10 μm.

only faint background staining in untransfected Cas-deficient fibroblasts with either αCas1 or αCas3 (data not shown).

These in situ (cytoskeleton stretching) (Figure 5B) and in vivo (intact cell spreading) (Figure 5C) results, together with the observed preference of αCas1 binding for extended CasSD in vitro (Figure 5A), suggest that the in vitro extension of CasSD causes the conformational change of CasSD that is relevant to the force-dependent conformational change of Cas protein in vivo. Therefore, the extension-dependent phosphorylation of CasSD in vitro (Figure 4) appears to be relevant to the force-dependent phosphorylation of Cas in vivo (Figures 1, 2, and 5C).

DISCUSSION

Tyrosine Phosphorylation of Cas Is Involved in Physiological Force Transduction

Cas appears to act as a force transducer in vivo, since the knockdown of Cas expression by siRNA significantly attenuated stretch-dependent Rap1 activity (Figure 2A) and overexpression of wild-type Cas, but not coexpression of the phosphorylation-defective Cas mutant (Cas15YF) enhanced stretch-dependent Rap1 activity (Figure 2B). Phosphorylation by SFK is critical since stretch-dependent Cas phosphorylation was inhibited by the SFK inhibitor CGP77675 (Figure 1A) and attenuated in SYF cells (Figures 1B and 1C). These findings conform to our previous observation of stretch-dependent Cas phosphorylation by SFK in cytoskeletal complexes (Triton cytoskeletons) (Tamada et al., 2004) and indicate that tyrosine phosphorylation of Cas upon cell stretching constitutes a significant pathway for stretch-dependent Rap1 activation in intact cells (Sawada et al., 2001).

Possible Mechanisms for Stretch-Increased Cas Phosphorylation

Although Src was shown to be mechanically activated using genetically engineered reporters (Wang et al., 2005), it is not clear how endogenous c-Src is activated or if it is indirectly activated by force. We observed that Src-dependent phosphorylation of Cas was significantly increased by stretching in c-Src-expressing SYF cells without causing Src kinase activation (Figures 1B and 1C). These findings suggest that activation of the kinase is not primarily responsible for stretch-dependent increase of Cas phosphorylation in vivo. Since the SFK inhibitor greatly attenuated the stretch-dependent increase of Cas phosphorylation (Figure 1A), stretch-dependent alteration of phosphatase activity is also unlikely to be the cause. Further, the tyrosine phosphatase inhibitor sodium orthovanadate did not inhibit stretch-dependent tyrosine phosphorylation of Cas in Triton cytoskeletons (Tamada et al., 2004).

It is unlikely that stretching causes the spatial interaction between the kinase and the substrate, considering the constraints that such a mechanism places on the geometry of the cytoskeleton (Tamada et al., 2004). Since a mechanical modification of the substrate (Cas) was sufficient to increase Cas phosphorylation in vitro, we have focused on the analysis of that possibility.

Extension of Cas by Cellular Force

Both the amino-terminal SH3 and carboxy-terminal Src-binding domains are required for Cas localization at focal adhesions (Nakamoto et al., 1997), where cellular force is expected to be concentrated, and force-dependent signaling involving tyrosine phosphorylation occurs (Geiger and Bershadsky, 2002; Tamada et al., 2004). Since different proteins are known to associate with SH3 and Src-binding domains of Cas (Defilippi et al., 2006), an individual Cas molecule would be anchored to the cytoskeleton-adhesion complex via two distinct sites. In addition, the SH3 domain of Cas binds to FAK (focal adhesion kinase) (Harte et al., 1996). FAK has a FERM (erythrocyte band *4.1*-ezrin-*r*adixin-*m*oesin) domain commonly found in actin-binding proteins (Lee et al., 2004), associates with an actin-binding protein, talin (Chen et al., 1995), and is involved in the dynamic variation in tyrosine phosphorylation within focal adhesions (Ballestrem et al., 2006). Thus, we speculate that the amino-terminal anchor of Cas to the focal adhesion complex is more closely linked to the actin cytoskeleton than the carboxy-terminal anchor and that Cas is subjected to traction forces generated by the actin cytoskeleton (Figure 6).

Although the structures of the SH3 and the serine-rich domains of Cas were reported (Briknarova et al., 2005; Wisniewska et al., 2005), no structural analysis of the substrate domain has been reported, and the structure prediction algorithms (available at the Network Protein Sequence Analysis site) do not give a clear prediction for the structure of Cas substrate domain. We speculate that the intramolecular interactions within the substrate domain constrain its conformation in the absence of traction force and that traction force is required to expose YxxP sites to kinases.

Because our model centers on extension of Cas, the magnitude of force needed for extension is a concern. The force per integrin molecule in the adhesion site was estimated to be on the order of 1 pN (Balaban et al., 2001; Jiang et al., 2003), an order of magnitude below the force needed to reversibly unfold single domains of proteins such as spectrin by AFM (atomic force microscope) (Fisher et al., 1999). However, it has been shown that the protein unfolding force depends exponentially on the loading rate (Carrion-Vazquez et al., 1999), and at a low loading rate, proteins can be unfolded by forces even orders of magnitude below the forces required for unfolding at a high loading rate (Merkel et al., 1999). Further, extension of Cas may not require the force needed to cause "unfolding," i.e., linearization of a mechanically stable distinct structure. Thus, extension of Cas probably can occur by physiological forces at focal contact sites (order of a few pN). Further details of force-dependent extension and phosphorylation of the Cas substrate domain in vitro as well as in vivo are under study.

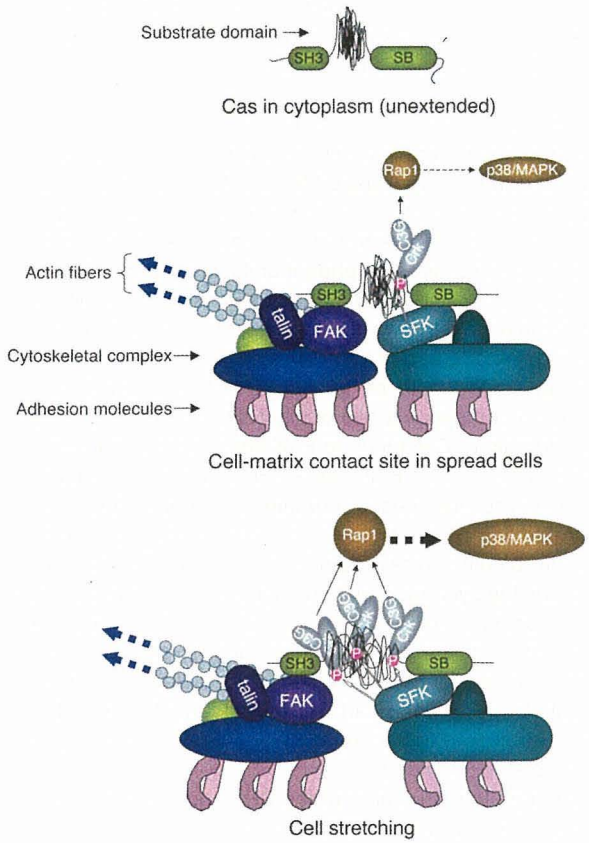

Figure 6. Model of Extension of Cas and Signaling at Cell-Matrix Contact Sites

The top and middle panels represent a Cas molecule with unextended configuration of substrate domain in the cytoplasm and a Cas molecule with moderate extension of substrate domain at the cell-matrix contact site of spread cells, respectively. The bottom panel represents the extension-dependent phosphorylation of the Cas substrate domain by SFK and enhancement of its downstream signaling. SH3 and SB represent the SH3- and the Src-binding domains of Cas, respectively.

Physiological Role of Extension and Phosphorylation of Cas in Force Transduction

Several different experimental approaches indicate that Cas extension plays a role in the direct sensing of traction forces in vivo. In vitro, extension of NC-biotinylated CasSD remarkably enhanced its phosphorylation by exogenous c-Src, FynT, or Abl1 (Figure 4). Extension of CaSD was confirmed by measuring the separation of two halves of YFP linked to the ends of the CasSD (Figure 3B). Stretch-dependent phosphorylation of Cas in cytoskeletons and in intact cells further supports the idea that it is involved in physiological force sensing. Antibody binding to epitopes exposed by extension in regions of higher traction forces shows that Cas is extended in vivo. Although many force-dependent effects are observed within cells, extension of Cas appears to be a primary force-sensing process and not part of a secondary force-response pathway, since extension-dependent phosphorylation of CasSD by active kinases was observed in vitro, where any extraneous biochemical interactions or signaling pathways were completely eliminated. While extracellular matrix proteins also respond to force by unfolding (Oberhauser et al., 2002) and exhibit different functional effects (Zhong et al., 1998), we show here that a cytoplasmic protein, Cas, has a gain of function upon cell stretching in terms of increase in phosphorylation and activation of Crk/C3G-Rap1 signaling.

A much greater percentage extension is required to observe the increase of in vitro phosphorylation of CasSD (Figure 4A, lanes 2–6) than the percentage of cell stretching to observe an increase of in vivo Cas phosphorylation (Figures 1 and 2). In vivo, cytoskeletal filaments will not stretch significantly, and cytoskeletal networks are believed to be strain hardened by cell-generated traction forces; therefore, molecular complexes at "stress-bearing" sites will be greatly extended upon even mild cell stretching. Moreover, cell traction forces will pre-extend the cytoskeleton-bound Cas molecules in spread cells even without stretching (Figure 6, middle). Thus, 10% stretching of intact cells can cause more than 10% extension of "unextended" Cas (Figure 6, top), since traction forces are concentrated at cell-matrix contact sites (Geiger and Bershadsky, 2002). In addition, αCas1 immunostaining shows that Cas is extended in the high-traction force regions of cells where Cas is phosphorylated (Figure 5C).

In other studies, shear stress increases Cas phosphorylation by SFK in vascular endothelial cells (Okuda et al., 1999). Since shear stress is known to modulate the cell contractility (Chien et al., 2005) in which Cas has been shown to play a role (Tang and Tan, 2003), extension of Cas caused by the increased cell contractility might result in shear stress-dependent phosphorylation. Thus, local extension of Cas is likely to be involved in the local response to various types of "mechanical stress" and can possibly account for the versatile function of Cas (Defilippi et al., 2006).

Substrate Priming as a General Mechanism of Cell Signaling

Enhancement of a substrate's susceptibility to phosphorylation by mechanical extension is designated as extension-dependent "substrate priming." The transduction of cell forces into a biochemical signal by mechanical substrate priming could be highly flexible and dynamic. The extent of substrate extension in vivo will depend upon the extent of strain produced locally in the cell, resulting in a graded extent of substrate phosphorylation and, consequently, gradations in the magnitude of downstream signaling events. Substrate priming by mechanical force might be generally involved in kinase signaling, particularly in light of our observation that a number of other cytoskeletal proteins are tyrosine phosphorylated in a stretch-dependent manner (Tamada et al., 2004) and since substrate conformation is a critical determinant in phosphorylation of other SFK substrates (Cooper et al., 1984). Thus, we suggest that substrate priming by localized protein

extension provides a simple mechanism for sensing the level of force on a cell as well as the location at which force is applied.

EXPERIMENTAL PROCEDURES

Antibodies

Polyclonal antibodies against Cas protein (αCas1, αCas2, and αCas3) were described previously (Sakai et al., 1994). The polyclonal anti-phospho-Cas antibodies pCas-165 and pCas-410, a polyclonal anti-phospho-SrcY416 antibody, and a polyclonal anti-phospho-SrcY527 antibody were purchased from Cell Signaling. The polyclonal anti-phospho-Cas antibody αP-Cas460Y (Miyake et al., 2005) was used for in vitro experiments with CasSD. Monoclonal anti-GFP (JL-8) and anti-RFP (anti-DsRed) antibodies were purchased from Clontech and BD Pharmingen, respectively. Monoclonal anti-Src (GD11) and anti-polyHistidine antibodies were purchased from Upstate Biotechnology and Sigma, respectively. Polyclonal anti-actin and anti-Rap1 antibodies were purchased from Santa Cruz Biotech.

Cells and DNA Plasmid Transfection

Human embryonic kidney (HEK) 293 cells, Cas-deficient fibroblasts (Huang et al., 2002), and SYF cells that lack c-Src, c-Yes, and Fyn were cultured in DMEM supplemented with 10% fetal bovine serum (FBS) and penicillin/streptomycin (100 IU/ml and 100 μg/ml) at 37°C and 5% CO_2. DNA plasmid transfection was performed with Fugene 6 (Roche) according to the manufacturer's protocol. To isolate stably transfected cell lines, pPUR that carried a puromycin-resistant gene (Clontech) was cotransfected, and clones were selected using puromycin (Clontech).

Immunoprecipitation and In Vitro Kinase Assay of Src

To measure the Src kinase activity in SYF cells and stable transfectant cells derived from SYF cells, Src was immunoprecipitated, and an in vitro kinase assay was performed using acid-treated enolase as a substrate. Phosphorylation of enolase was analyzed by anti-phospho-tyrosine immunoblotting. Details of the in vitro kinase assay of immunoprecipitated Src are described in the Supplemental Data section.

RNA Interference Experiments

To decrease the endogenous expression of Cas protein, two different siRNAs, BCAR1-HSS114272 and BCAR1-HSS114273 (Stealth RNAi, Invitrogen), were transfected into HEK293 cells (1×10^5/dish) using Lipofectamine RNAiMAX according to the manufacturer's protocol (180 pmol RNA interference [RNAi] and 9 μl Lipofectamine RNAiMAX/dish) (Invitrogen). Six hours after transfection, culture medium was replaced with fresh DMEM containing 10% FBS. Twenty-four hours after transfection, cells were either stretched or left unstretched and subjected to biochemical analyses.

Quantification of Rap1 Activity

A GST pull-down assay was performed to measure the Rap1 activity using GST-RalGDS-RBD that preferentially bound to Rap1·GTP (Sakakibara et al., 2002). To measure the Rap1 input, equivalent portions of each lysate were directly subjected to SDS-PAGE followed by immunoblotting.

Kinases and Substrates

Recombinant c-Src, FynT, Abl1, Csk, and ZAP-70 were purchased from Invitrogen. Specific kinase activities of c-Src, FynT, Csk, and ZAP-70 were determined by an in vitro kinase assay using poly-Glu/Tyr (4:1) as a substrate (Invitrogen). Abl1 kinase activity was determined by an in vitro kinase assay using Abl1 substrate (Invitrogen). Enolase (rabbit muscle) was purchased from Sigma. Bacterially expressed cdb3 was used as a substrate to measure the ZAP-70 activity.

Preparation of Biotinylated Proteins

Various forms of biotinylated CasSD were prepared using Biotin AviTag technology (Avidity). The Biotin AviTag sequence consists of 15 residues (GLNDIFEAQKIEWHE) and is specifically and efficiently biotinylated by the protein biotin ligase BirA. Biotinylated AviTag-fused proteins were obtained by coexpression with BirA in bacteria (BL21 Star, Invitrogen) cultured in NZCYM medium containing d-biotin (50 μM; Research Organics) at the time of IPTG induction. The molar ratio of biotin to AviTag-fused protein was confirmed to be 2:1 in NC-biotinylated CasSD and NY/CY-NC-biotinylated CasSD, and 1:1 in C-biotinylated CasSD and NY/CY-C-biotinylated CasSD. Details of biotinylated protein preparation are given in the Supplemental Data section.

For chimeric proteins of biotinylated CasSD and YFP components (NY/CY-NC-biotinylated CasSD and NY/CY-C-biotinylated CasSD), yellow fluorescence was observed and estimated in bacteria and in solution by quantitative fluorescence microscopy. Solutions containing NY/CY-NC-biotinylated CasSD or NY/CY-C-biotinylated CasSD were as fluorescent as solutions containing bacterially expressed full-length YFP at the same concentration (0.8 μM).

Plasmids

Plasmids used in this work are described in the Supplemental Data section.

Stretching of Intact Cells

Cells plated on collagen (type I; Sigma-Aldrich)-coated stretchable silicone dishes (Sawada et al., 2001) were either stretched biaxially (and kept stretched) or left unstretched in our cell stretching system (Sawada et al., 2001; Tamada et al., 2004).

Covalent Avidin Coating of Latex Membrane and Preparation of Biotinylated Proteins Specifically Bound to Avidin-Coated Latex Membrane

Avidin (Neutravidin) was covalently immobilized onto the surface of latex membrane by introducing the amine-reactive groups using Friedal-Crafts chemistry, and biotinylated proteins were bound to the immobilized avidin. Details of preparation of biotinylated protein bound to latex membrane are described in the Supplemental Data section.

IPE System

A biotinylated protein-bound latex membrane set in an adjustable tension ring was placed on a lubricated round-shaped glass stage and stretched biaxially and uniformly by pulling down the tension ring (Figure 3A, bottom). Magnitude of the latex membrane stretching was described as percent change of length in each dimension. For example, 100% stretching represented 2-fold expansion in each dimension. To recover the protein for analysis, the protein-bound membrane (Figure 3A, bottom) was incubated with 1× SDS sample buffer containing 0.12 M DTT at 95°C for 5 min. Using amine-reactive, photocleavable biotin analog (NHS-PC-LC-Biotin, PIERCE) (Sawada and Sheetz, 2002), we confirmed that this procedure recovered the majority (>95%) of biotinylated proteins bound to the immobilized avidin.

YFP Amino-Terminal Swapping Assay

NY/CY-NC-biotinylated, NY/CY-C-biotinylated (Figure 3B), or NC-biotinylated CasSD (Figure 3A) bound to avidin-coated latex membrane was prepared as described above. After stretching of latex membrane (100%) or without stretching, biotinylated CasSD proteins were washed two times with 1% BSA and 1% Triton X-100 in PBS and incubated with 2 μM His_6-YFP-N in 1% BSA and 1% Triton X-100 in PBS containing 1 mM DTT for 10 min at room temperature. The bound protein complex on the latex membrane was washed four times with 1% BSA and 1% Triton X-100 in PBS and two times with 1% Triton X-100 in PBS, recovered with 1× SDS sample buffer containing 0.12 M DTT. The samples were subjected to SDS-PAGE followed by anti-polyHistidine immunoblotting and avidin affinity blotting.